Electronic Supplementary Material (ESI) for Chemical Communications.

Supporting Information for:

Redox-active ligand promoted electrophile addition at cobalt

Minzhu Zou and Kate M. Waldie*

Department of Chemistry and Chemical Biology, Rutgers, The State University of New Jersey
123 Bevier Road, Piscataway, New Jersey 08854, United States

*Corresponding author: kate.waldie@rutgers.edu

Table of Contents

Experimental Details

General Considerations. All reactions were performed under anaerobic and anhydrous conditions using a Vacuum Atmospheres glovebox or Schlenk techniques unless otherwise specified. All solvents were dried using a Pure Process Technology Solvent Purification System and/or activated 3Å molecular sieves. Acetonitrile (MeCN), tetrahydrofuran (THF), diethyl ether (Et_2O), pentane, and hexanes were also degassed on a high-vacuum Schlenk line with at least three freeze-pump-thaw cycles and stored in a N_2-filled glovebox. Deuterated solvents were purchased from Cambridge Isotope Labs. THF-d_8 was used as received; CD_3CN was degassed and stored over 3Å molecular sieves under N_2 atmosphere unless otherwise noted.

5-(Trifluoromethyl)-5H-dibenzo[b,d]thiophen-5-ium trifluoromethanesulfonate ([DBT–CF_3]OTf), 5-(trifluoromethyl)-5H-thianthren-5-ium trifluoromethanesulfonate ([Thi–CF_3]OTf), diphenyl(trifluoromethyl)sulfonium trifluoromethanesulfonate ([Ph_2S–CF_3]OTf), 3-methyl-1*H*-indole, and *N*-fluorobenzenesulfonimide (NFSI) were purchased from Ambeed, Inc. and used as received. Iodine (I_2, resublimed crystals), 2,2,6,6-tetramethylpiperidine-*N*-oxyl radical (TEMPO), and potassium bromide (KBr) were purchased from Fisher Scientific or Sigma-Aldrich and used as received. *N*-iodosuccinimide (NIS) was purchased from Sigma-Aldrich and recrystallized from 1,4-dioxane/CCl_4 to give a white crystalline solid. Cobaltocene was purchased from Strem Chemicals and sublimed under high vacuum at 50-60 °C prior to use. Ferrocene (Fc) was purchased from Sigma-Aldrich and recrystallized from hexanes prior to use. Tetra-*n*-butylammonium hexafluorophosphate ([^{n}Bu$_4$N][PF_6]) was purchased from Sigma-Aldrich, recrystallized from ethanol, and dried under vacuum for at least 48 h prior to use. [CpCo(^{iPr}opda)] **1** was synthesized according to literature procedure.[1]

All NMR spectra were collected at 25 °C unless otherwise noted. ^{1}H and ^{13}C{^{1}H} NMR spectra were recorded using Bruker 500 MHz NMR spectrometer. The chemical shifts of ^{1}H, ^{13}C nuclei are reported in ppm and referenced to the residual solvent peaks (^{1}H NMR) or the characteristic resonances of the solvent nuclei (^{13}C{^{1}H} NMR) as internal standards. All ^{19}F NMR spectra were referenced to fluorobenzene (δ = –113.15 ppm). Electronic absorption spectra were recorded on an Agilent Cary 60 UV-vis spectrophotometer with Cary WinUV software using a 1 cm path length quartz cuvette. Infrared (IR) spectra were recorded on a Bruker Vertex 80 FT-IR spectrometer with a liquid nitrogen cooled MCT detector. High resolution mass spectra (HRMS) were collected using an electrospray ionization (ESI) source on positive ion mode with a Xevo™ G2-XS QTof mass spectrometer. Continuous wave EPR spectra were recorded at ambient and liquid nitrogen temperatures on an X-band Bruker EMXPlus spectrometer equipped with an EMX standard resonator and a Bruker PremiumX microwave bridge. The spectra were simulated using EasySpin for MATLAB.[2]

Electrochemistry. Cyclic voltammetry (CV) studies were performed using a BASi Epsilon EClipse potentiostat, and the data were processed using BASi Epsilon-EC software (version 2.13.77). All experiments were performed under N_2 in a 20 mL glass vial with a glassy carbon (GC) working electrode (3 mm diameter, BASi), Pt wire counter electrode, and Ag/$AgNO_3$

reference electrode. The GC electrode was polished with alumina (0.05 μm, BASi) prior to use. All potentials are referenced to the $Fc^{+/0}$ couple using ferrocene (Fc) as an internal standard.

Spectroelectrochemistry (SEC). SEC data were recorded on an Agilent Cary 60 UV-vis spectrophotometer using a Specac® Omni Cell with PTFE spacer (ca. 0.2 mm) under N_2. Sample solutions were prepared in MeCN with [^{n}Bu$_4$N][PF_6] (0.2 M) and cobalt complex (4 mM). The Pt mesh working electrode, Pt mesh counter electrode, and Ag wire pseudo-reference electrode (BioLogic) were placed in the thin-layer solution. The Pt electrodes were cleaned with HNO_3 prior to use. UV-vis SEC was carried out using linear sweep voltammetry at 1 mV/s while acquiring UV-vis spectra from 1000-200 nm at fast scan rate (4800 nm/min).

X-ray Crystallography. Single crystal X-ray diffraction (SC-XRD) frames were collected on a Rigaku XTALab Synergy-S single crystal diffractometer equipped with a HyPix-6000HE area detector (hybrid photon counting) using a Kappa 4-circle goniometer with a Cu/Kα radiation (λ = 1.54184 Å). Crystals were mounted on a cryo-loop under a mixture of paraffin and Paratone-N oil, and all data were collected at 100 K using an Oxford nitrogen gas 800 Series cryostream system (Rigaku). The X-ray data were corrected for Lorenz effects and polarization. Multi-scan or Gaussian absorption correction was applied in the SADABS[3] or CrysAlisPRO[4] program. The structures were solved by an intrinsic phasing method with SHELXT.[5] All non-hydrogen atoms were refined with SHELXL[6] based on F_{obs}^2. All hydrogen atom coordinates were calculated with idealized geometries. Scattering factors (f_o, f', f'') are as described in SHELXL. Additional crystallographic data and final R indices are given in Tables S2. All structures have been deposited into the Cambridge Structural Database (CCDC 2286968-2286970).

Computational Details. All calculations were performed within the Gaussian 16 Revision A.03 package[7] using the def2-TZVPP basis set for Co and the def2-TZVP basis set for all other atoms.[8] Initial geometry for optimization was obtained from the coordinates of the crystal structure of **3**. The ground-state structure was optimized in the gas phase on an ultrafine grid with the opt = tight keyword. Harmonic vibrational frequency calculation was performed to ensure no imaginary frequencies were present for the optimized structures. Spin density diagram was visualized on a grid of 80^3 points within GaussView 6.0.16 at an isovalue of 0.005.

Synthesis and Characterization

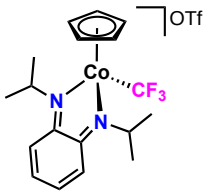

[CpCo(^{iPr}bqdi)(CF_3)]OTf (2). An oven-dried 20 mL vial with a stir bar was charged with [CpCo(^{iPr}opda)] **1** (31 mg, 99 µmol), [DBT−CF_3]OTf (38.5 mg, 96 µmol), and dry MeCN (5 mL). The red mixture was stirred for 30 min, and the solvent was evaporated under vacuum. The remaining solid was washed with hexanes (3 × 2 mL) and recrystallized by layering Et_2O/hexanes (8 mL/8 mL) upon a cobalt solution (0.8 mL) in MeCN at –35 °C. A light red supernatant was removed by pipette, and a dark red crystalline solid was washed with hexanes and dried under vacuum. Complex **2** is stable as a solid or in solution over extended time periods. Isolated yield: 48.5 mg, 95%. Red block single crystals suitable for X-ray diffraction were obtained via layering Et_2O/pentane (1:1) upon a cobalt solution in MeCN at –35 °C.

^{1}H NMR (CD_3CN, 25 °C, 500 MHz) δ 7.31-7.27 (m, 2H, Ar-*H*), 7.01-6.97 (m, 2H, Ar-*H*), 5.78 (s, 5H, C_5H_5), 4.89 (hept, ^3J = 7.0 Hz, 2H, C*H*), 1.75 (d, ^3J = 7.1 Hz, 6H, CH_3), 1.50 (d, ^3J = 7.0 Hz, 6H, CH_3). ^{13}C{^{1}H} NMR (CD_3CN, 25 °C, 126 MHz) δ 170.2 (*C*=N), 133.4 and 122.3 (C_{arom}H), 93.6 (C_5H_5), 67.3 (C_{alkyl}H), 22.7 and 22.6 (*C*H_3). ^{19}F NMR (CD_3CN, 25 °C, 471 MHz) δ -7.03 (s, 3F, CF_3), -78.27 (br s, 3F, SO_3CF_3). UV-vis (MeCN, $M^{-1}\cdot cm^{-1}$): 207 nm (ε = 26,540), 248 nm (ε = 13,380), 285 nm (sh, ε = 6,080), 409 nm (ε = 6,370), 518 nm (br, ε = 2,820). FT-IR (KBr pellet, cm^{-1}): 3100 (m), 2985 (w), 2946 (w), 2886 (w), 1656 (w), 1625 (w), 1551 (w), 1534 (w), 1461 (m), 1427 (m), 1375 (m), 1270 (s, br), 1225 (m), 1160 (s), 1122 (m), 1032 (s, br), 951 (w), 895 (w), 863 (m), 836 (w), 808 (w), 758 (m), 709 (w). HRMS: Calcd for $C_{18}H_{23}CoF_3N_2$ ([**2** – OTf]$^+$): *m/z* 383.1140. Found: *m/z* 383.1126.

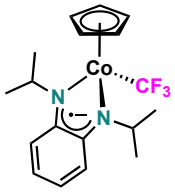

[CpCo(^{iPr}s-bqdi)(CF_3)] (3). An oven-dried 20 mL vial with a stir bar was charged with **2** (22 mg, 41 µmol), cobaltocene (7.5 mg, 40 µmol), and dry MeCN (4 mL). The red-brown mixture was stirred for 10 min, and the solvent was evaporated under vacuum. The product was extracted into hexanes, filtered through a Celite column, and dried under vacuum. Further purification was performed through recrystallization by slow pentane evaporation at –35 °C. Complex **3** is stable as a solid or in solution over extended time periods. Isolated yield: 13.8 mg, 91%. Dark block single crystals suitable for X-ray diffraction were obtained via slow evaporation of a cobalt solution in pentane at –35 °C.

UV-vis (MeCN, $M^{-1}\cdot cm^{-1}$): 223 nm (ε = 27,550), 306 nm (ε = 7,680), 401 nm (ε = 9,510), 482 nm (ε = 2,890), 551 nm (sh, ε = 2,270), 753 nm (sh, ε = 860), 844 nm (ε = 1,200), 961 nm (ε = 1,240). FT-IR (KBr pellet, cm^{-1}): 3110 (w), 3076 (w), 2977 (m), 2934 (m), 2875 (w), 1656 (w), 1619 (w), 1570 (w), 1525 (m), 1462 (m, br), 1406 (w), 1383 (w), 1363 (m), 1341 (m), 1312 (m), 1261 (w), 1178 (w), 1155 (s), 1115 (s), 1051 (s, br), 1016 (s), 997 (s), 839 (m), 806 (m), 728 (s), 704 (w), 695 (w). HRMS: Calcd for $C_{18}H_{23}CoF_3N_2$ ([**3**]$^{\bullet+}$): *m/z* 383.1140. Found: *m/z* 383.1199. Effective Magnetic Moment: μ_{eff} = 1.86 μB (Evans method).

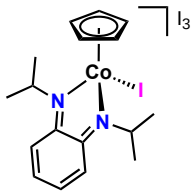

[CpCo(^{iPr}bqdi)(I)]I_3 (5). An oven-dried Schlenk flask with a stir bar was charged with **1** (12.7 mg, 40 μmol) and THF (5 mL) in the N_2-filled glovebox. Under N_2 flow, iodine (I_2, 22.8 mg, 90 μmol) was added as a dark crystalline solid. The dark pink solution turned dark brown in seconds, and the mixture was stirred for another hour. Solvent and excess I_2 were removed under vacuum. The remaining dark brown solid was washed with Et_2O and dried under vacuum. The crude product was further purified by recrystallization from THF/hexanes. Isolated yield: 31.7 mg, 95%. Dark block single crystals suitable for X-ray diffraction were obtained via layering hexanes upon a cobalt solution in THF/Et_2O at –35 °C.

^{1}H NMR (CD_3CN, 25 °C, 500 MHz) δ 7.31-7.28 (m, 2H, Ar-*H*), 6.91-6.87 (m, 2H, Ar-*H*), 5.84 (s, 5H, C_5H_5), 5.32 (hept, ^3J = 6.9 Hz, 2H, C*H*), 1.90 (d, ^3J = 7.0 Hz, 6H, CH_3), 1.71 (d, ^3J = 7.0 Hz, 6H, CH_3). ^{1}H NMR (THF-d_8, 25 °C, 500 MHz) δ 7.45-7.43 (m, 2H, Ar-*H*), 6.96-6.94 (m, 2H, Ar-*H*), 6.06 (s, 5H, C_5H_5), 5.41 (hept, ^3J = 6.9 Hz, 2H, C*H*), 2.04 (d, ^3J = 7.0 Hz, 6H, CH_3), 1.80 (d, ^3J = 7.0 Hz, 6H, CH_3). ^{13}C{^{1}H} NMR (THF-d_8, 25 °C, 126 MHz) δ 170.9 (*C*=N), 133.5 and 122.0 (C_{arom}H), 90.5 (C_5H_5), 67.7 (C_{alkyl}H), 25.7 and 25.6 (*C*H_3).

X-ray Data and Structures

X-ray Crystallographic Data

Table S1. Selected angles (°) and bond lengths (Å) for complexes **2**, **3**, and **5**.

	2	**3**	**5**
N1–Co1–N2	83.5(2)	84.01(6)	82.70(13)
Co1–N1	1.899(3)	1.9057(16)	1.946(3)
Co1–N2	-	1.8990(15)	1.908(3)
Co1–*C*F$_3$/*I*	1.956(6)	1.924(2)	2.5875(6)
Co1–Cp$_{centroid}$	1.709	1.745	1.709
N1–C1	1.311(5)	1.346(2)	1.316(5)
N2–C6	-	1.343(2)	1.303(5)

Table S2. Crystal data and structure refinement for complexes **2**, **3**, and **5**.

	2	**3**	**5**
CCDC Number	2286969	2286970	2286968
Empirical formula	$C_{19}H_{23}CoF_6N_2O_3S$	$C_{18}H_{23}CoF_3N_2$	$C_{17}H_{23}CoI_4N_2$
Formula weight	532.39	383.31	821.93
Temperature (K)	100(2)	100(2)	100(2)
Wavelength (Å)	1.54184	1.54184	1.54184
Crystal shape, color	Block, red	Block, black	Block, black
Crystal size (mm^3)	0.17 × 0.06 × 0.04	0.23 × 0.07 × 0.05	0.11 × 0.06 × 0.03
Crystal system	Orthorhombic	Monoclinic	Monoclinic
Space group	$Pmn2_1$	$P2_1/n$	$P2_1/n$
a (Å)	10.9754(5)	9.2280(3)	8.55250(7)
b (Å)	9.2478(5)	18.9005(6)	11.72077(9)
c (Å)	11.0627(5)	10.1686(3)	22.80175(18)
α (deg)	90	90	90
β (deg)	90	108.165(3)	97.4775(7)
γ (deg)	90	90	90
Volume ($Å^3$)	1122.85(9)	1685.16(10)	2266.25(3)
Z	2	4	4
Density (calculated) (Mg/m^3)	1.575	1.511	2.409
Absorption coefficient (mm^{-1})	7.541	8.278	48.731
Max. and min transmission	1.000 and 0.5585	1.000 and 0.290	1.000 and 0.527
F(000)	544	796	1512
Reflections collected	14152	22800	30732
Independent reflections	2204	3139	4620
Completeness to θ = 67.684°	100.0%	100.0%	100.0%
Restraints / parameters	1 / 159	0 / 221	1 / 225
R(int)	0.0365	0.0391	0.0478
Final R indices [I > 2σ(I)]	R_1 = 0.0340 wR_2 = 0.0853	R_1 = 0.0306 wR_2 = 0.0719	R_1 = 0.0284 wR_2 = 0.0759
Largest diff. peak and hole (e $Å^{-3}$)	0.622 and -0.685	0.720 and -0.266	1.500 and -1.202
Goodness-of-fit on F^2	1.088	1.052	1.058
Flack parameter	-0.029(3)		-

X-ray Structures

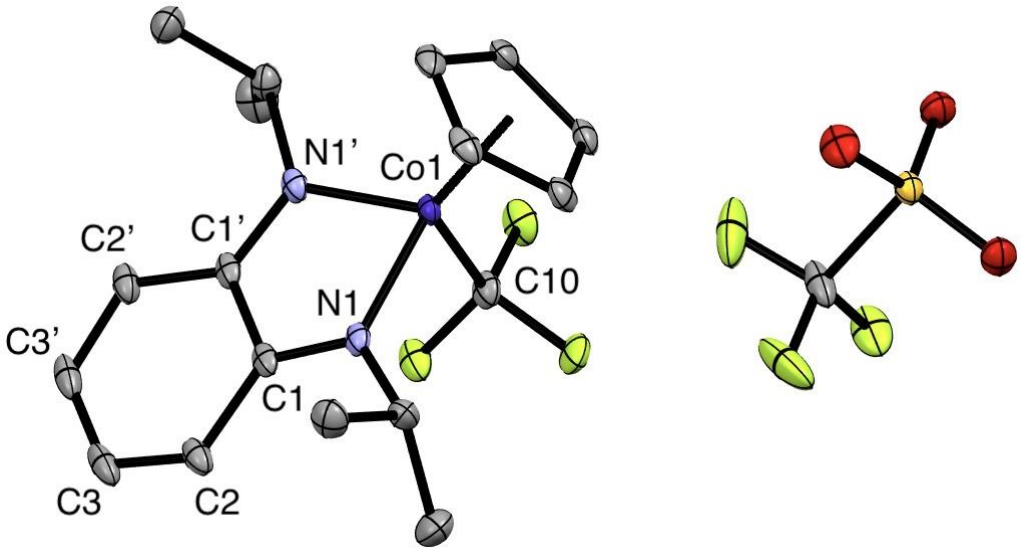

Figure S1. Single crystal X-ray structure of **2** shown with 30% probability ellipsoids. Hydrogen atoms are omitted for clarity. Selected bond distances (Å): Co1–$Cp_{centroid}$ = 1.709; Co1–N1 = 1.899(3); Co1–C10 = 1.956(6); N1–C1 = 1.311(5); C1–C2 = 1.437(6); C1–C1' = 1.468(8); C2–C3 = 1.348(6); C3–C3' = 1.435(11). Selected angles (°): N1–Co1–N1' = 83.5(2).

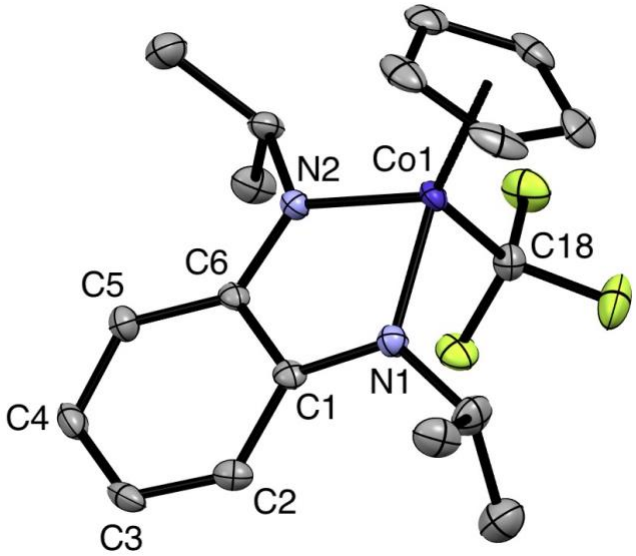

Figure S2. Single crystal X-ray structure of **3** shown with 50% probability ellipsoids. Hydrogen atoms are omitted for clarity. Selected bond distances (Å): Co1–$Cp_{centroid}$ = 1.745; Co1–N1 = 1.9057(16); Co1–N2 = 1.8990(15); Co1–C18 = 1.924(2); N1–C1 = 1.346(2); N2–C6 = 1.343(2); C1–C2 = 1.420(3); C1–C6 = 1.449(3); C2–C3 = 1.375(3); C3–C4 = 1.404(3); C4–C5 = 1.371(3); C5–C6 = 1.424(3). Selected angles (°): N1–Co1–N2 = 84.01(6).

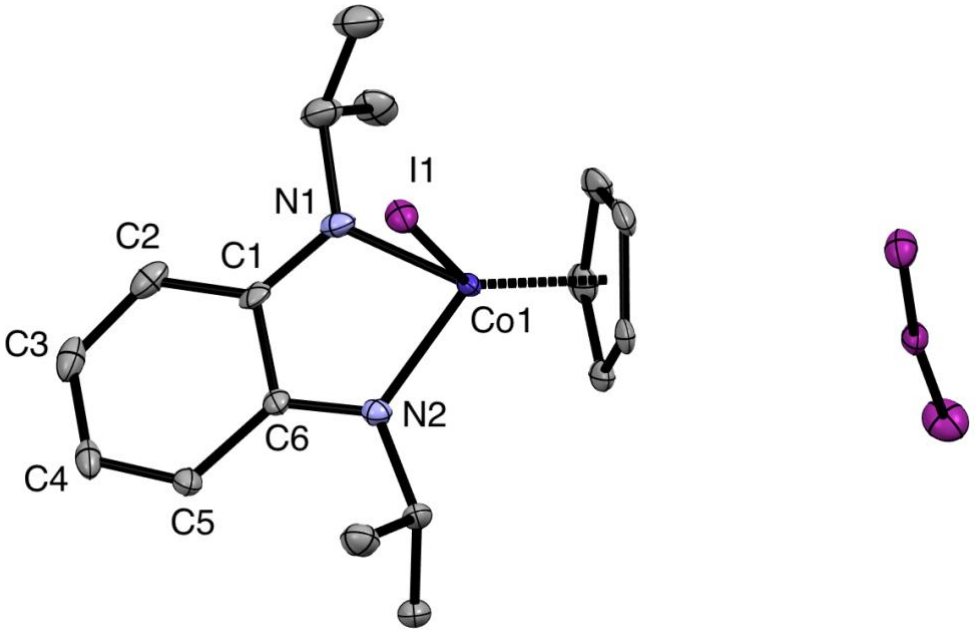

Figure S3. Single crystal X-ray structure of **5** shown with 50% probability ellipsoids. Hydrogen atoms are omitted for clarity. Selected bond distances (Å): Co1–$Cp_{centroid}$ = 1.709; Co1–I1 = 2.5875(6); Co1–N1 = 1.946(3); Co1–N2 = 1.908(3); N1–C1 = 1.316(5); N2–C6 = 1.303(5); C1–C2 = 1.454(5); C1–C6 = 1.472(5); C2–C3 = 1.349(6); C3–C4 = 1.438(6); C4–C5 = 1.353(5); C5–C6 = 1.446(5). Selected angles (°): N1–Co1–N2 = 82.70(13).

NMR Data

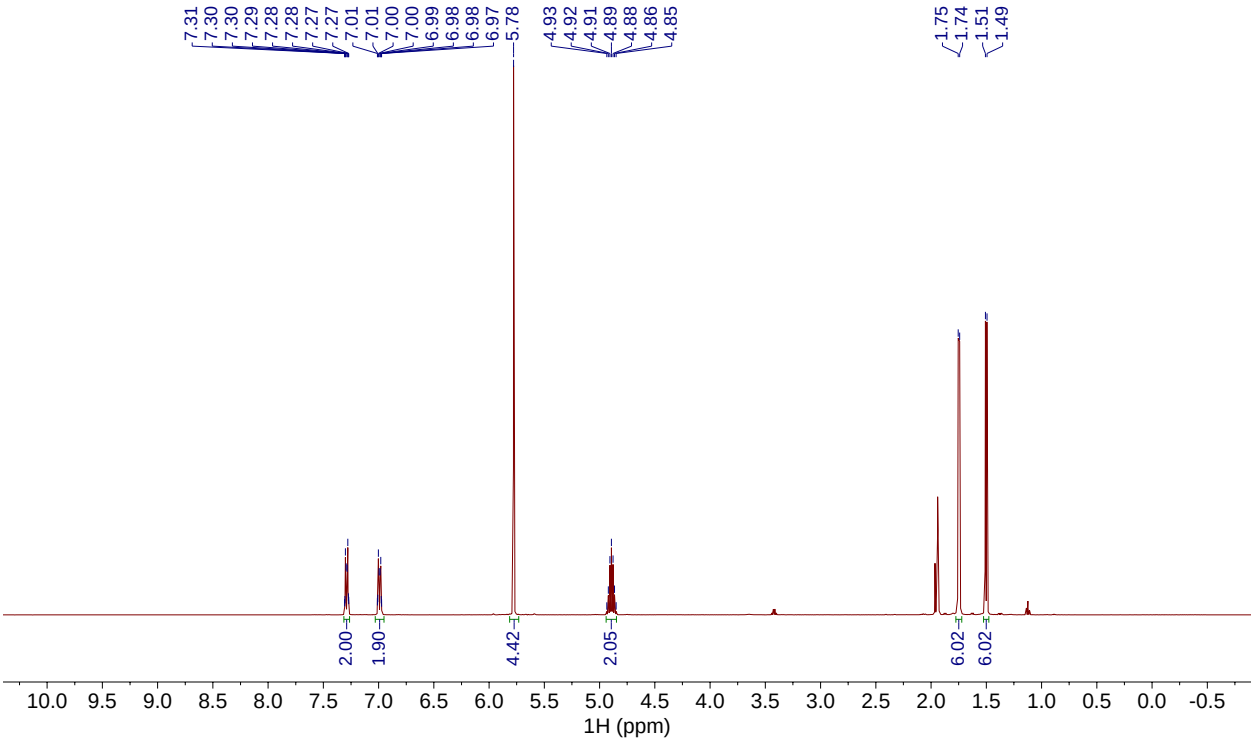

Figure S4. ^{1}H NMR spectrum of **2** in CD_3CN.

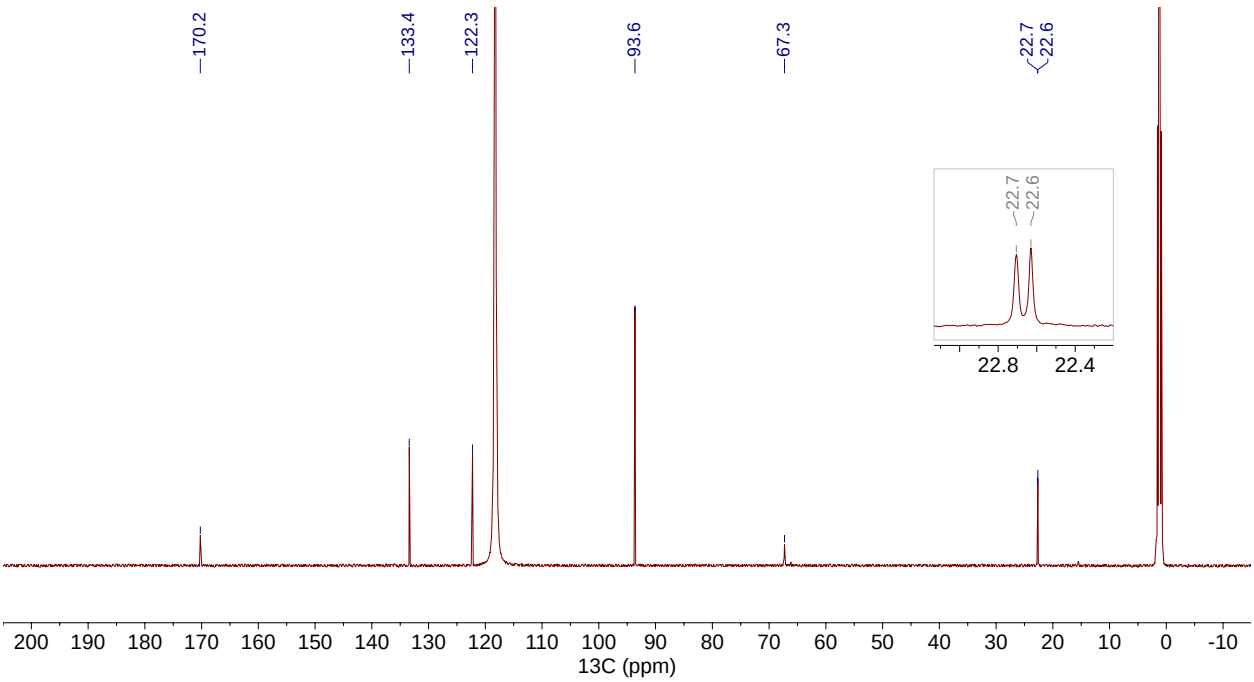

Figure S5. $^{13}C\{^{1}H\}$ NMR spectrum of **2** in CD_3CN. The signal of the CF_3 moiety is not visible due to coupling with the quadrupolar ^{59}Co nucleus and the ^{19}F nuclei.

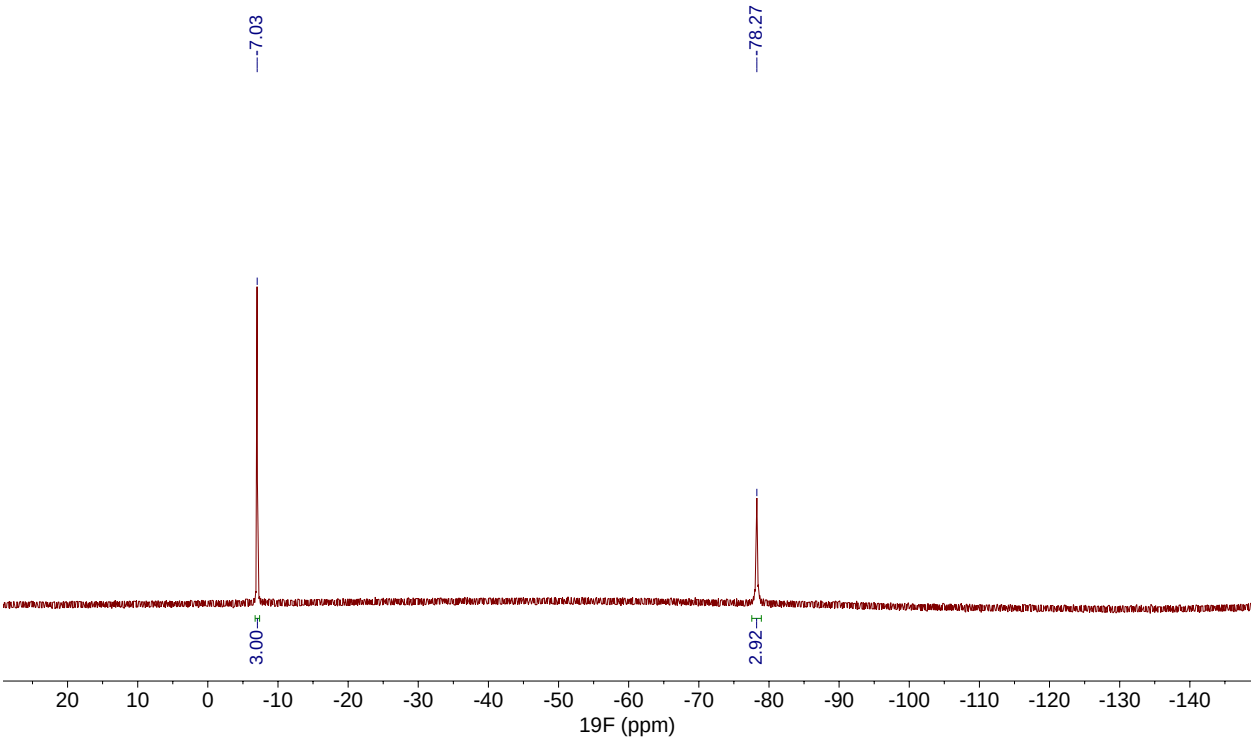

Figure S6. ^{19}F NMR spectrum of **2** in CD_3CN.

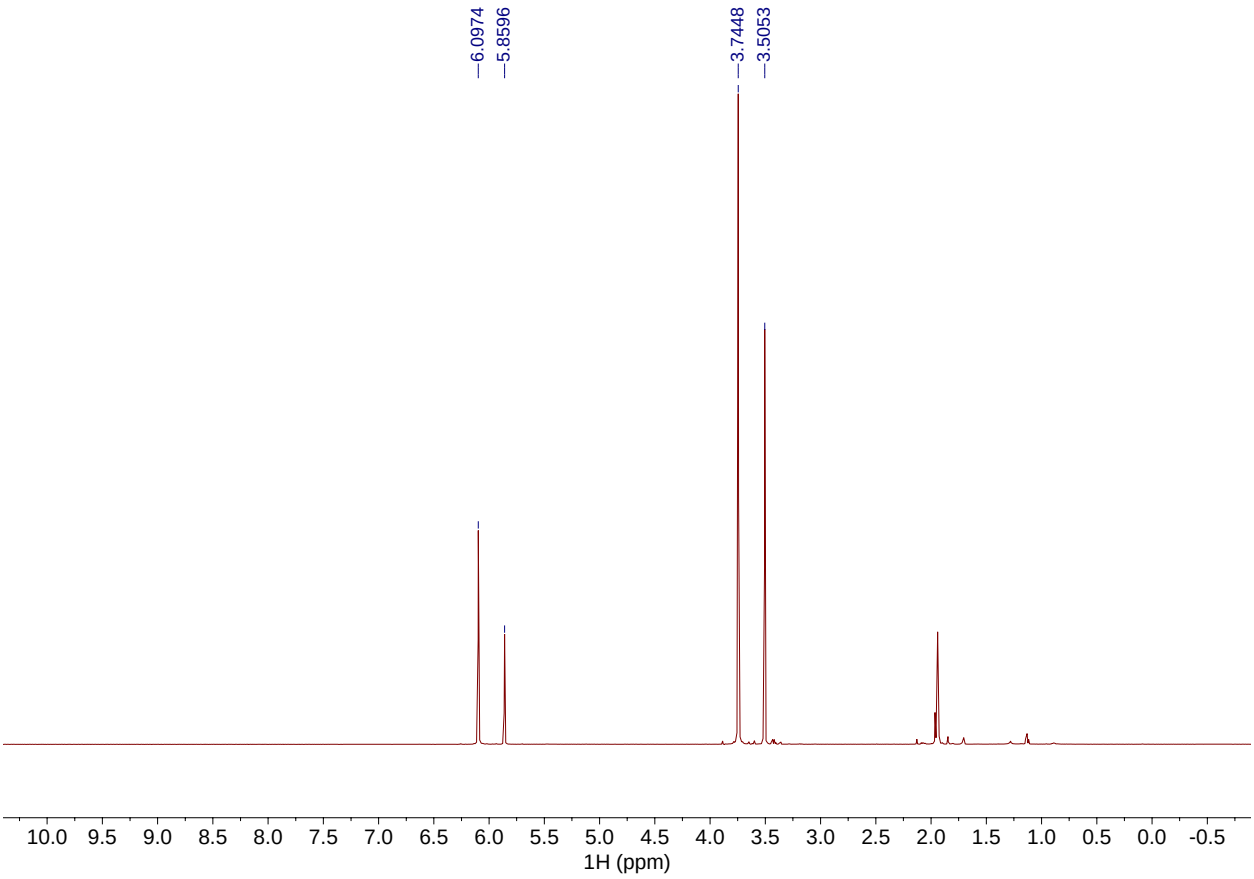

Figure S7. Magnetic moment measurement of **3** by Evans method in CD_3CN at 25 °C with 1,3,5-trimethoxybenzene as the internal standard. [**3**] = 0.039 M, Δf = 119 Hz, f = 500.15 MHz, μ_{eff} = 1.86 μB.

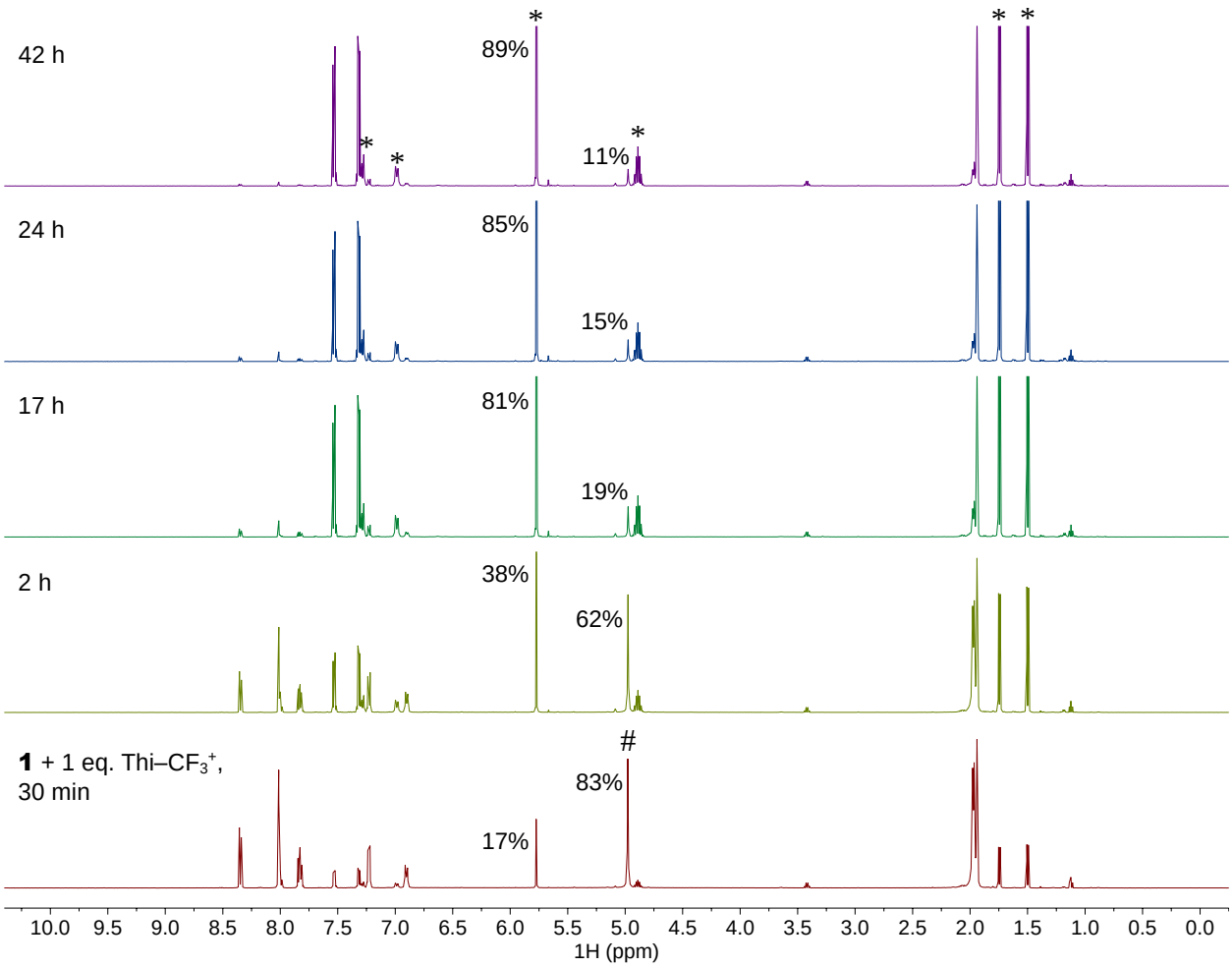

Figure S8. Monitoring the reaction of **1** and 1 equiv. [Thi–CF_3]OTf in CD_3CN by ^1H NMR over 42 h. # = **1**. * = **2**. Percentages of **1** and **2** based on integrations of the corresponding Cp signal.

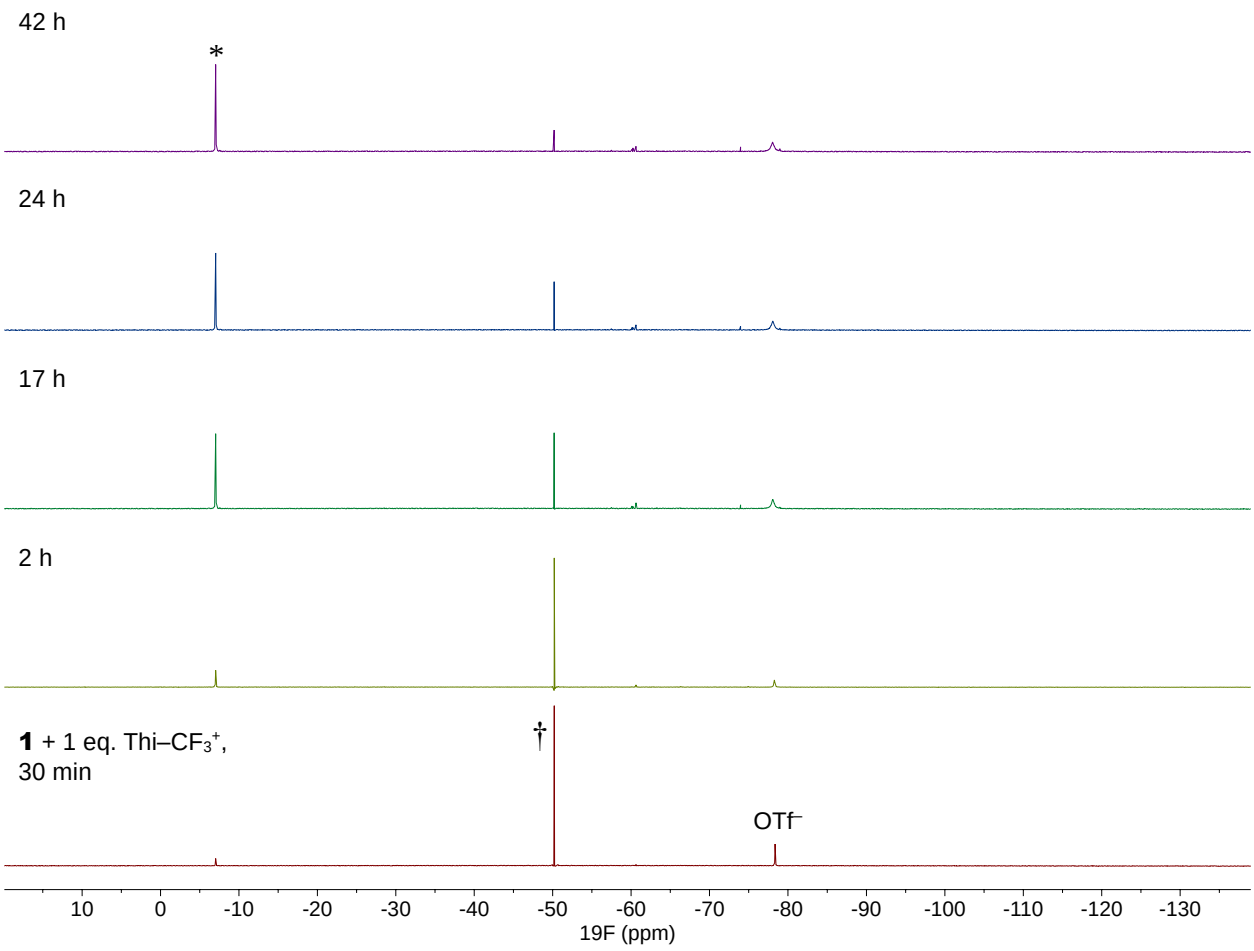

Figure S9. Monitoring the reaction of **1** and 1 equiv. [Thi–CF_3]OTf in CD_3CN by ^{19}F NMR over 42 h. † = $[Thi–CF_3]^+$. * = **2**.

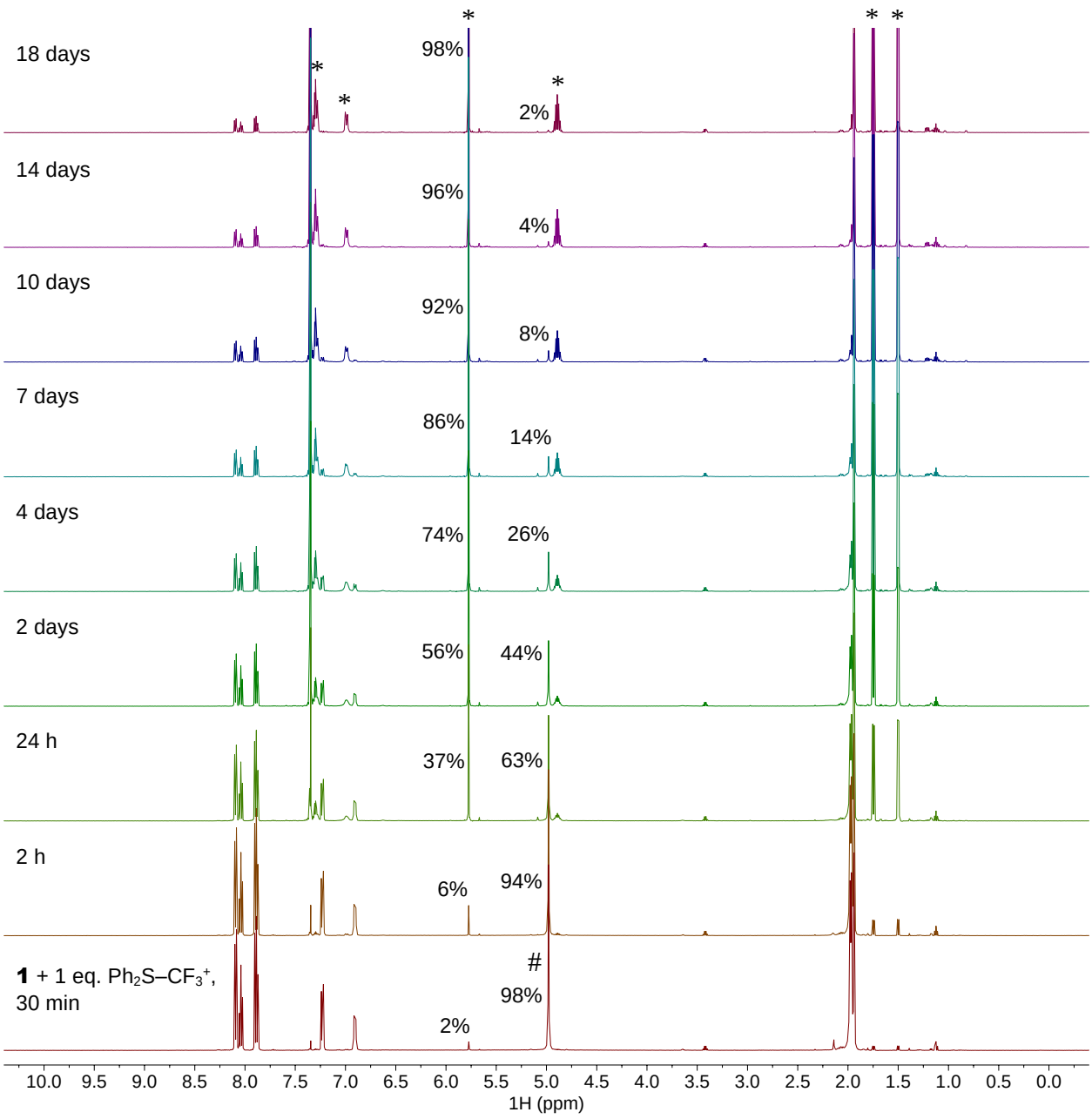

Figure S10. Monitoring the reaction of **1** and 1 equiv. [$Ph_2S–CF_3$]OTf in CD_3CN by ^1H NMR over 18 days. # = **1**. * = **2**. Percentages of **1** and **2** based on integrations of the corresponding Cp signal.

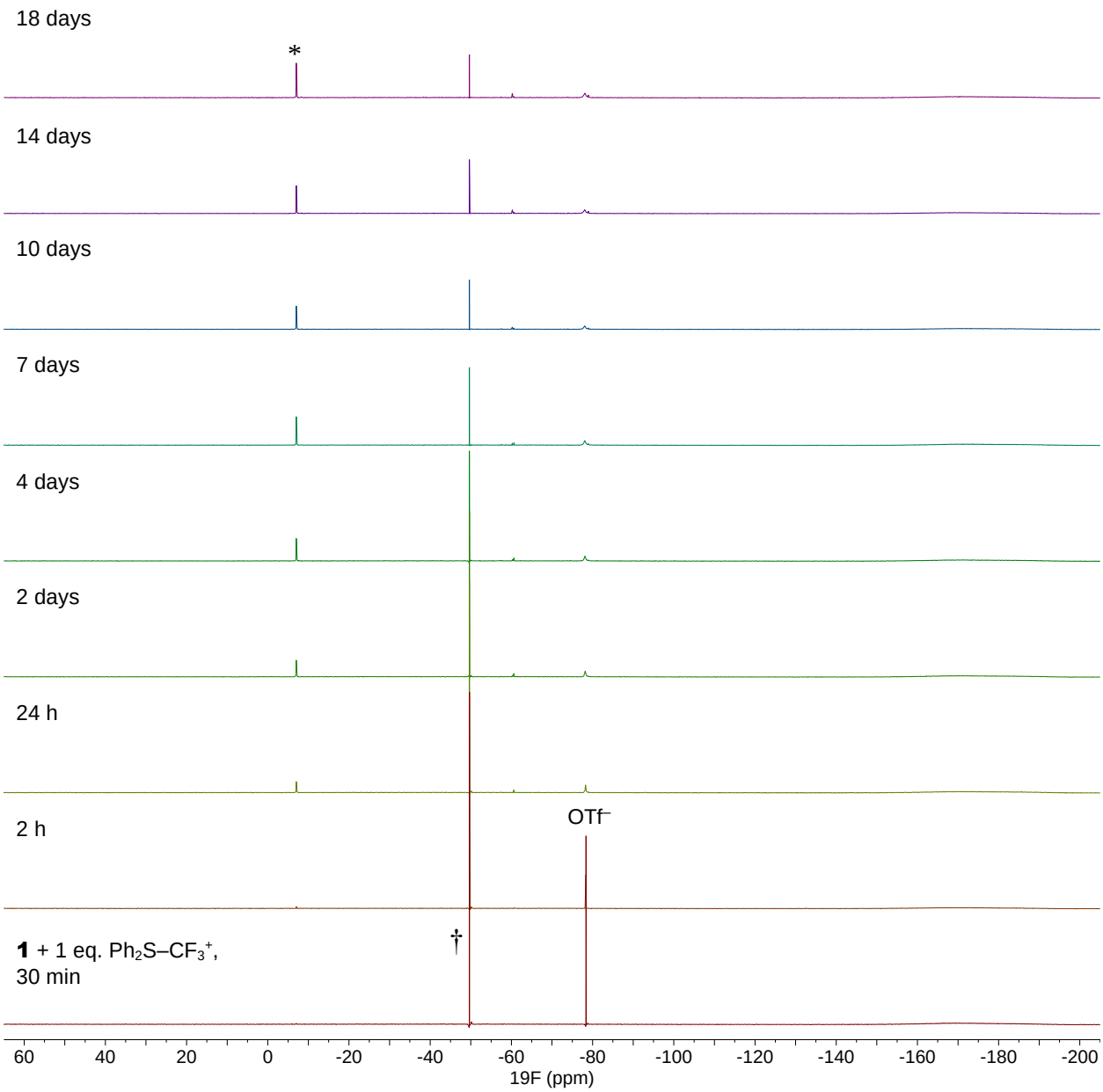

Figure S11. Monitoring the reaction of **1** and 1 equiv. [$Ph_2S–CF_3$]OTf in CD_3CN by ^{19}F NMR over 18 days. † = $[Ph_2S–CF_3]^+$. * = **2**.

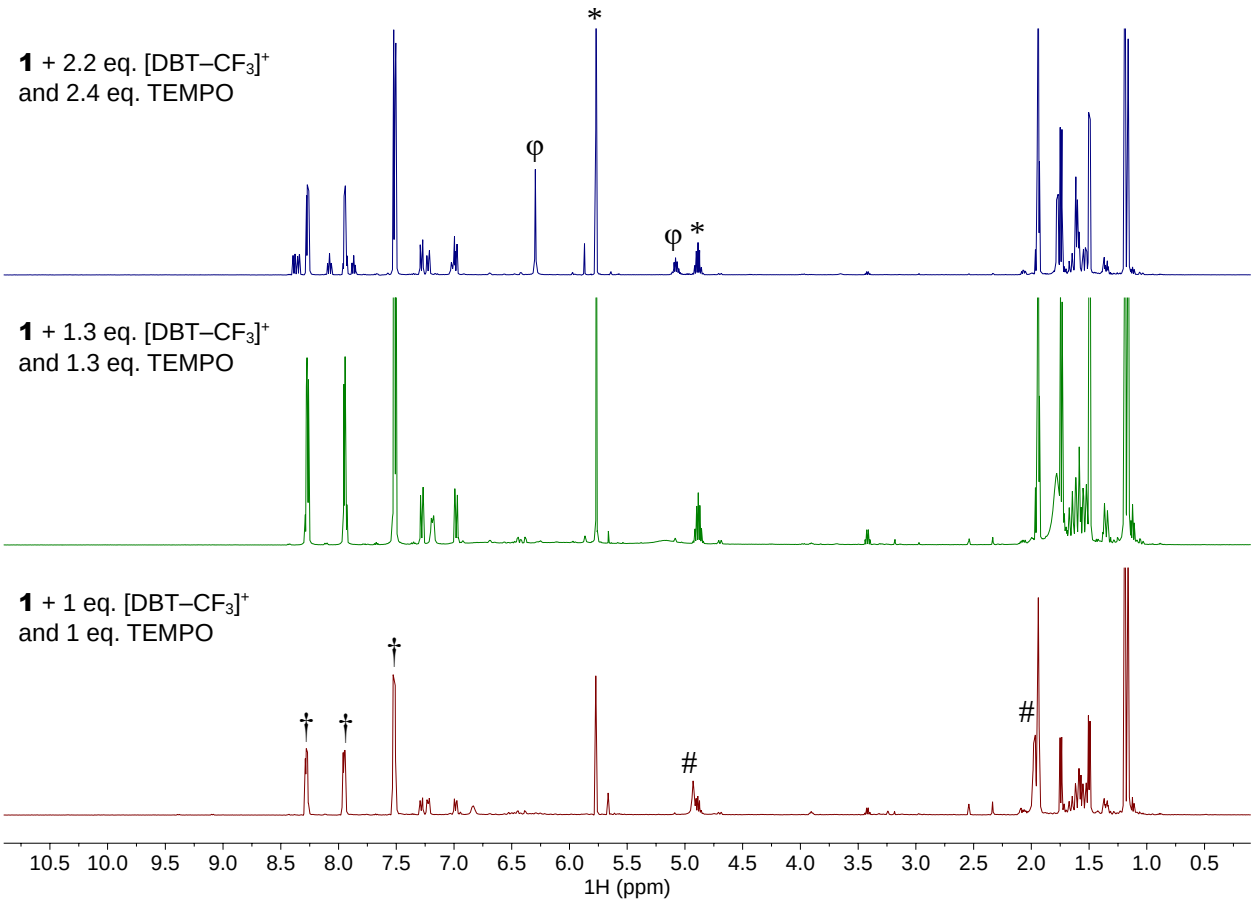

Figure S12. ^{1}H NMR spectrum for the reaction of **1** with [DBT–CF_3]OTf and TEMPO in CD_3CN. # = **1**. * = **2**. φ = **[1–MeCN]$^{2+}$**. † = dibenzothiophene.

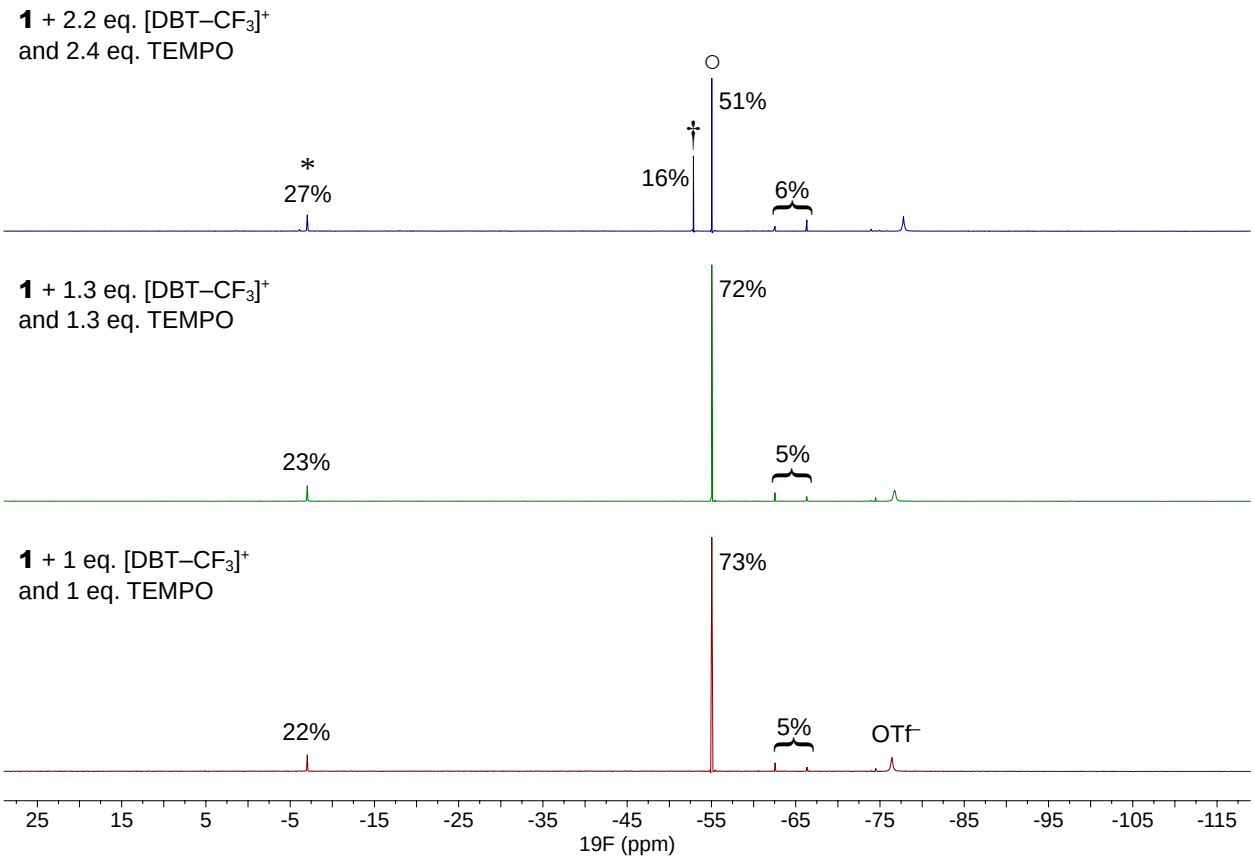

Figure S13. ^{19}F NMR spectrum of the mixture of **1** with [DBT–CF_3]OTf and TEMPO in CD_3CN. * = **2**. ○ = TEMPO–CF_3. † = $[DBT–CF_3]^+$. A relaxation delay of at least 6 seconds was used for acquiring ^{19}F NMR spectra.

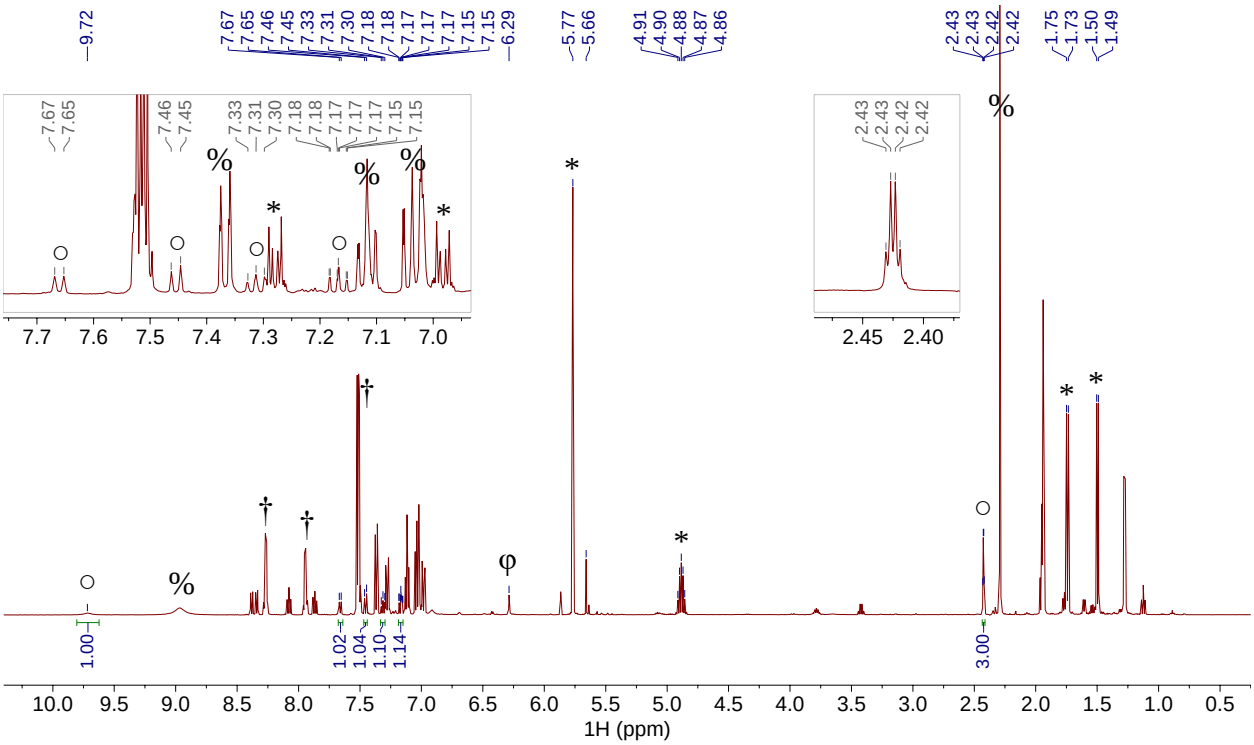

Figure S14. ^{1}H NMR spectrum for the reaction of **1** with 2.2 equiv. [DBT–CF_3]OTf and 2.4 equiv. 3-methyl-1*H*-indole in CD_3CN. * = **2**. φ = **[1–MeCN]$^{2+}$**. ○ = 3-methyl-2-(trifluoromethyl)-1*H*-indole. † = [DBT–CF_3]$^{+}$ or dibenzothiophene. % = 3-methyl-1*H*-indole.

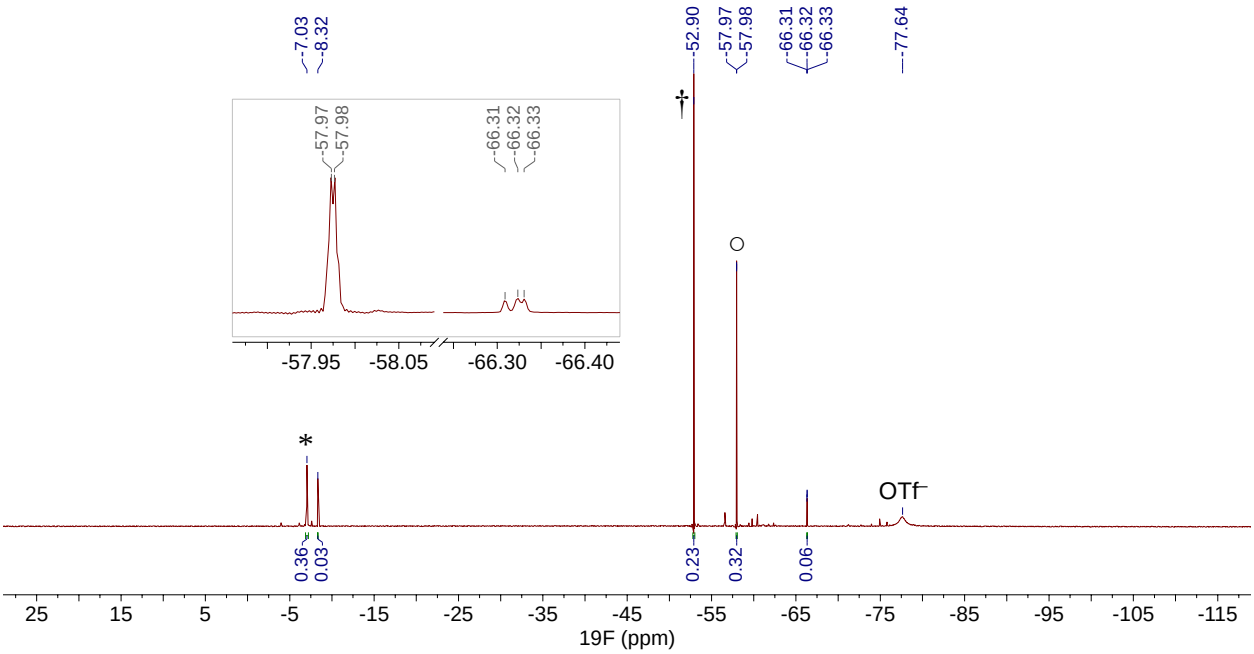

Figure S15. ^{19}F NMR spectrum of the mixture of **1** with 2.2 equiv. [DBT–CF_3]OTf and 2.4 equiv. 3-methyl-1*H*-indole in CD_3CN. * = **2**. ○ = 3-methyl-2-(trifluoromethyl)-1*H*-indole. † = [DBT–CF_3]$^{+}$. A relaxation delay of 6 seconds was used for acquiring ^{19}F NMR spectrum.

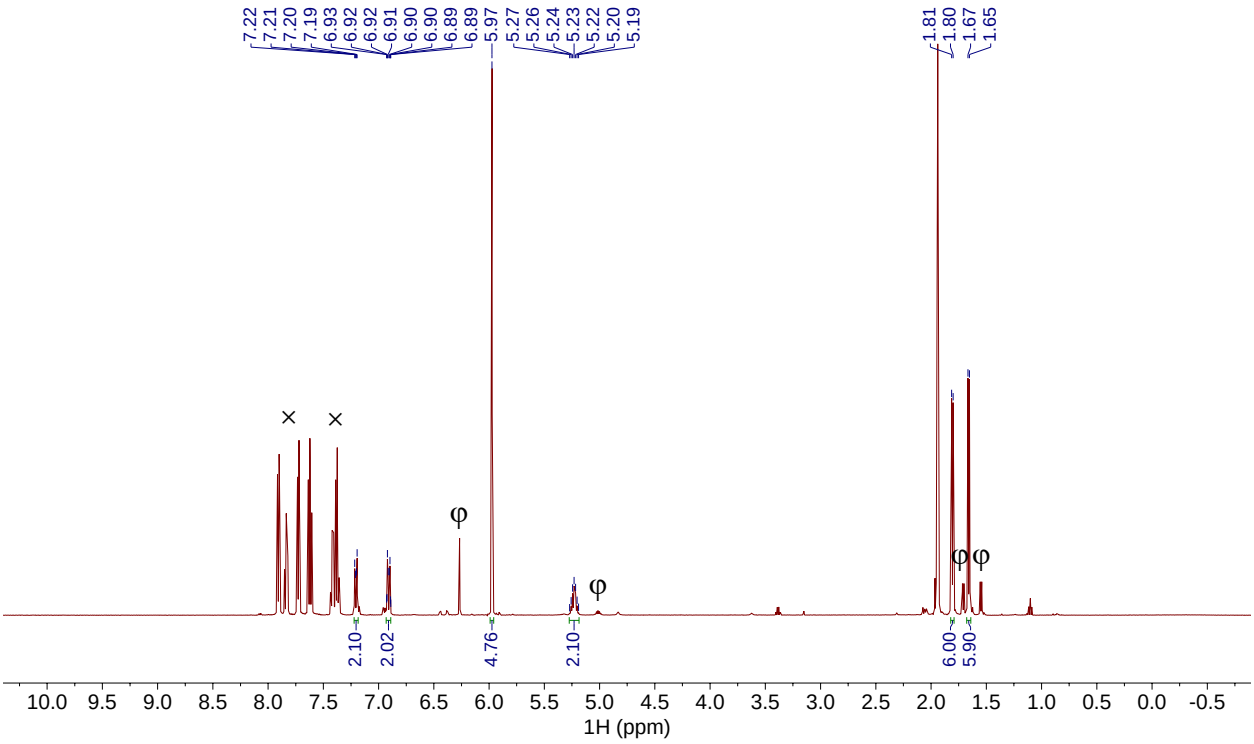

Figure S16. ^{1}H NMR spectrum of **4** in CD_3CN at –25 °C, synthesized *in-situ* via reaction of **1** and NFSI. φ = **[1–MeCN]$^{2+}$**. × = NFSI.

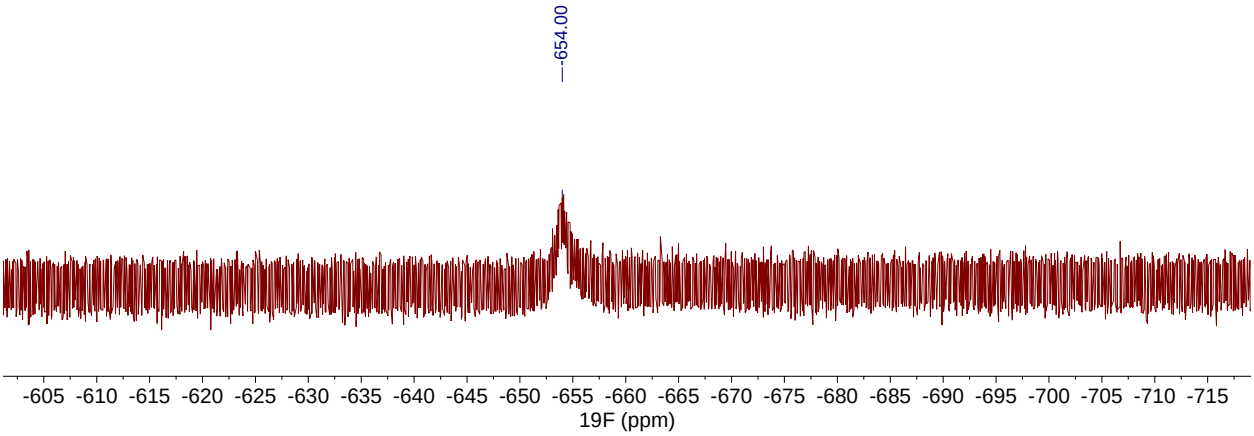

Figure S17. ^{19}F NMR spectrum of **4** in CD_3CN at –25 °C, synthesized *in-situ* via reaction of **1** and NFSI. This chemical shift is comparable to the reported CpCo–*F* analogues.[9]

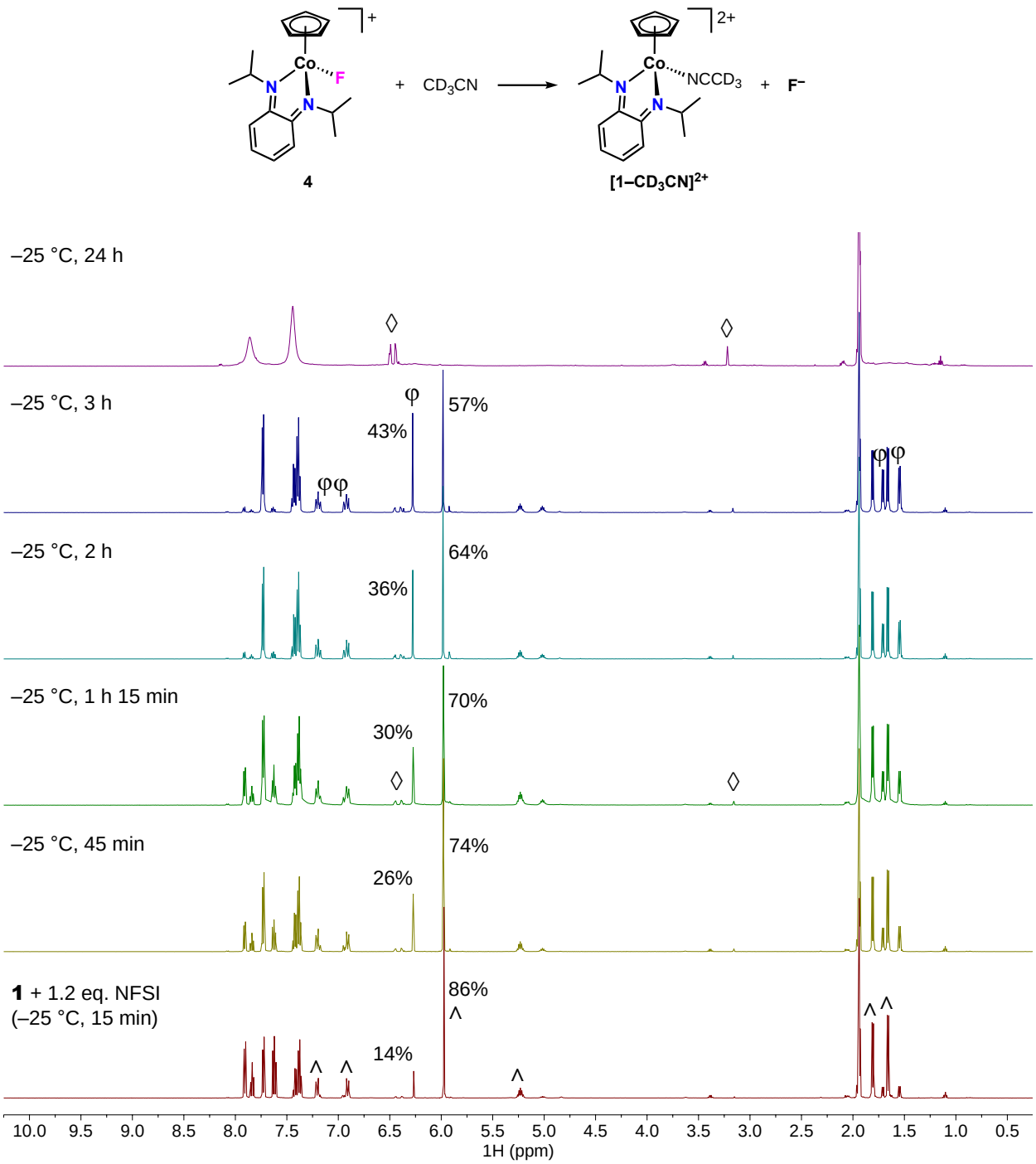

Figure S18. Monitoring the reaction of complex **1** and 1.2 equiv. NFSI in CD_3CN at –25 °C by ^1H NMR over 24 h. ^ = **4**. φ = **[1–MeCN]$^{2+}$**. Percentages of **4** and **[1−MeCN]$^{2+}$** based on integrations of the corresponding Cp signal. The NMR solution was cooled in a dry ice/o-xylene bath before sample injection and kept at –25 °C between spectrum acquisition. ◊ = CpD.

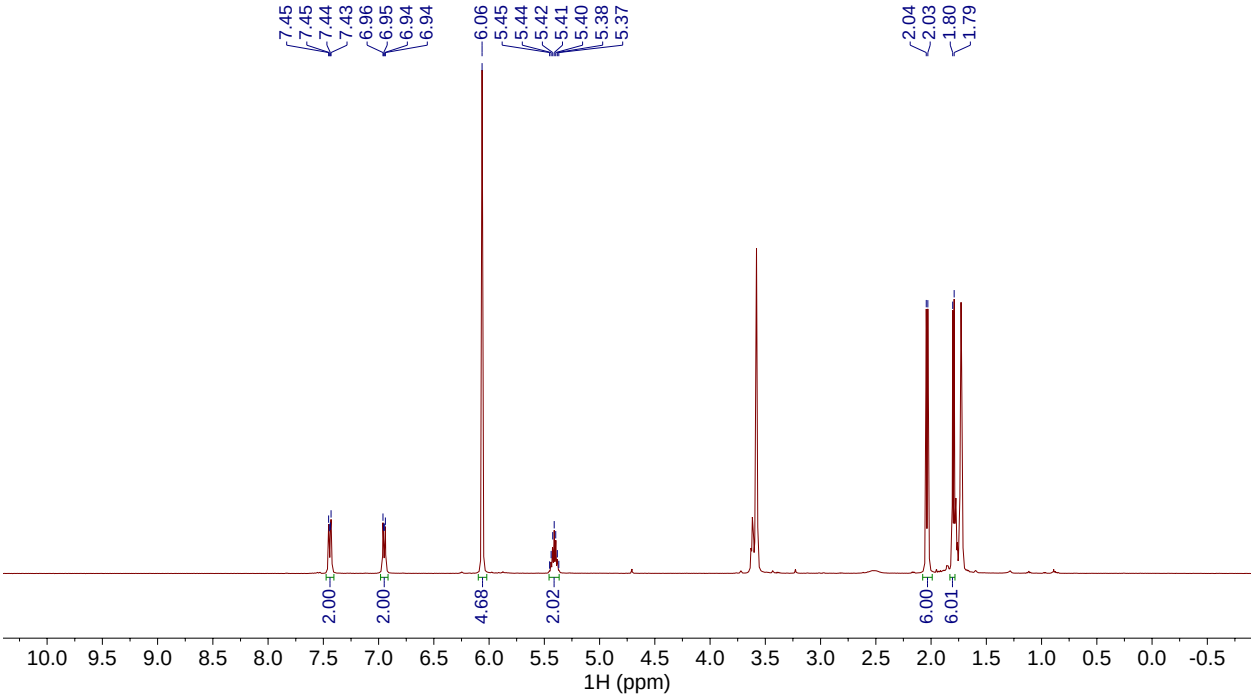

Figure S19. ^{1}H NMR spectrum of **5** in THF-d_8.

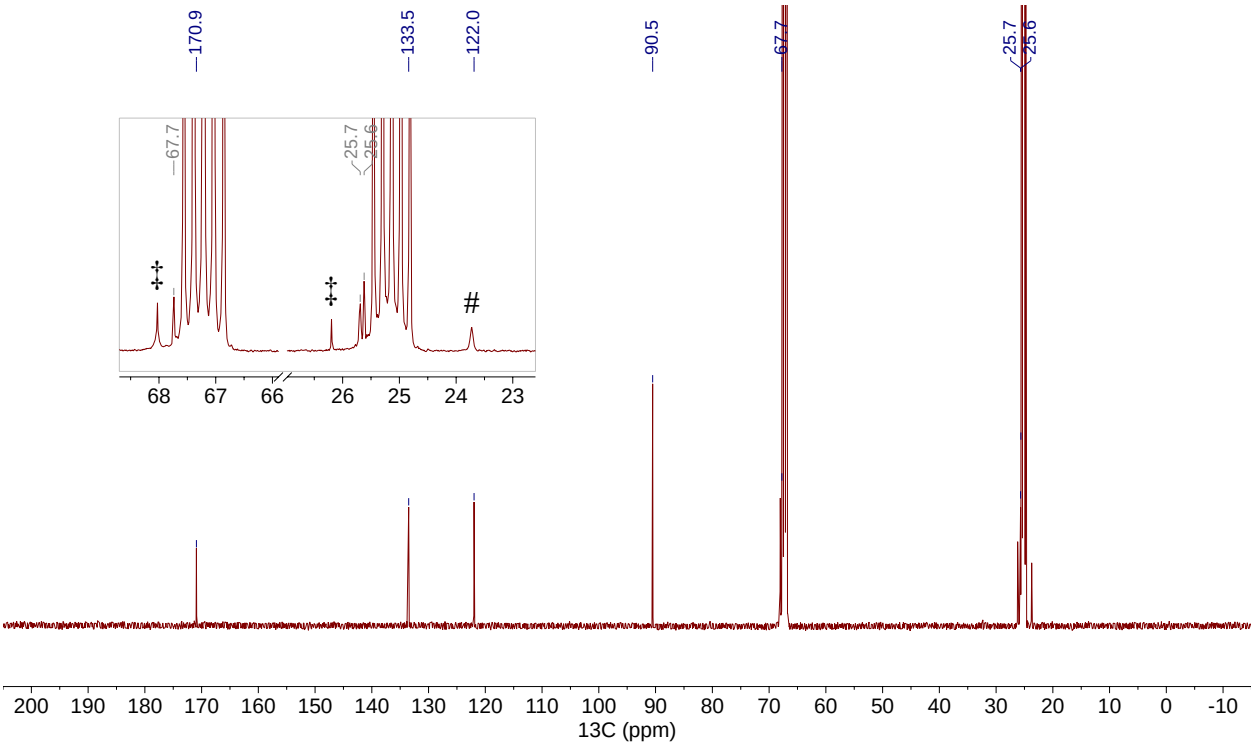

Figure S20. $^{13}C\{^{1}H\}$ NMR spectrum of **5** in THF-d_8. ‡ = THF. # = unknown.

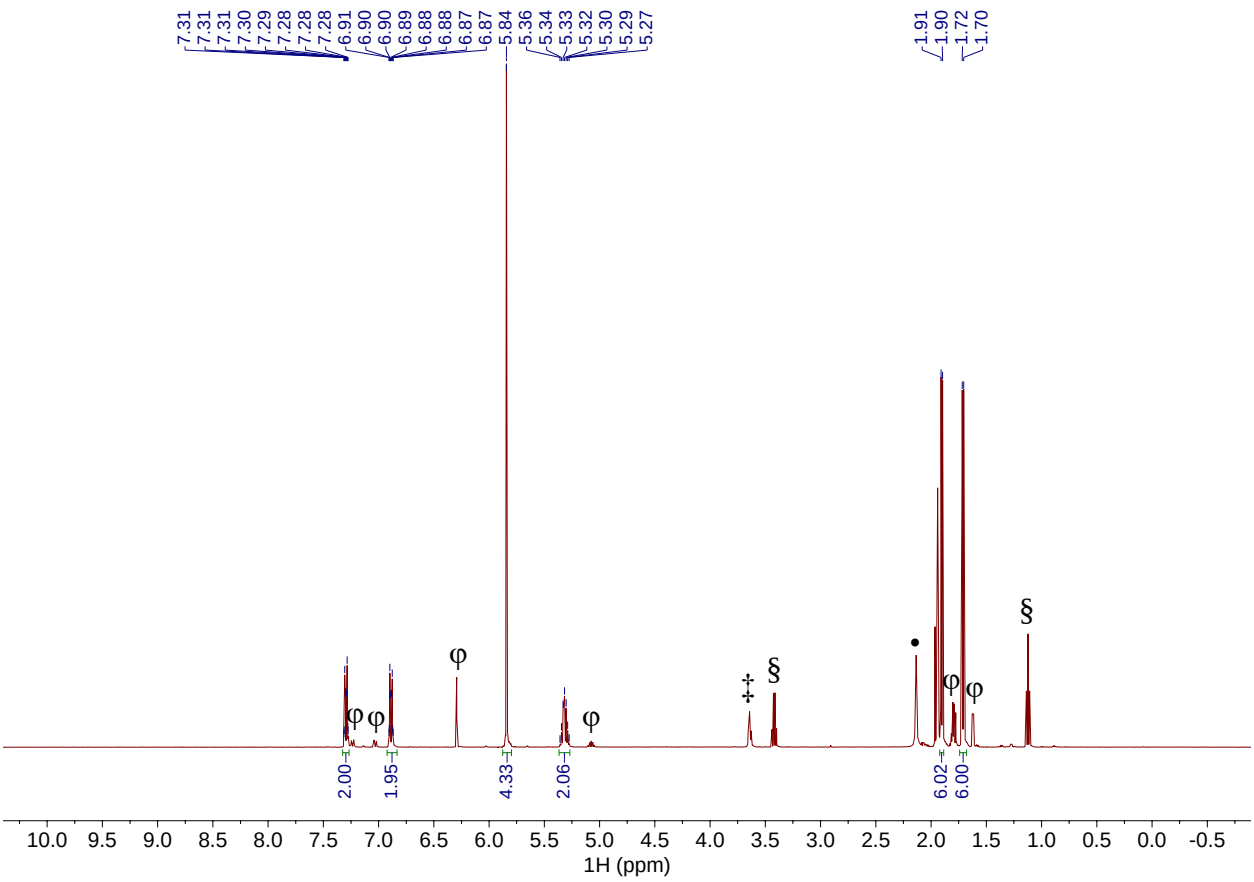

Figure S21. ^{1}H NMR spectrum of **5** in CD_3CN. φ = **[1–MeCN]$^{2+}$**. ‡ = THF. § = Et_2O. • = H_2O.

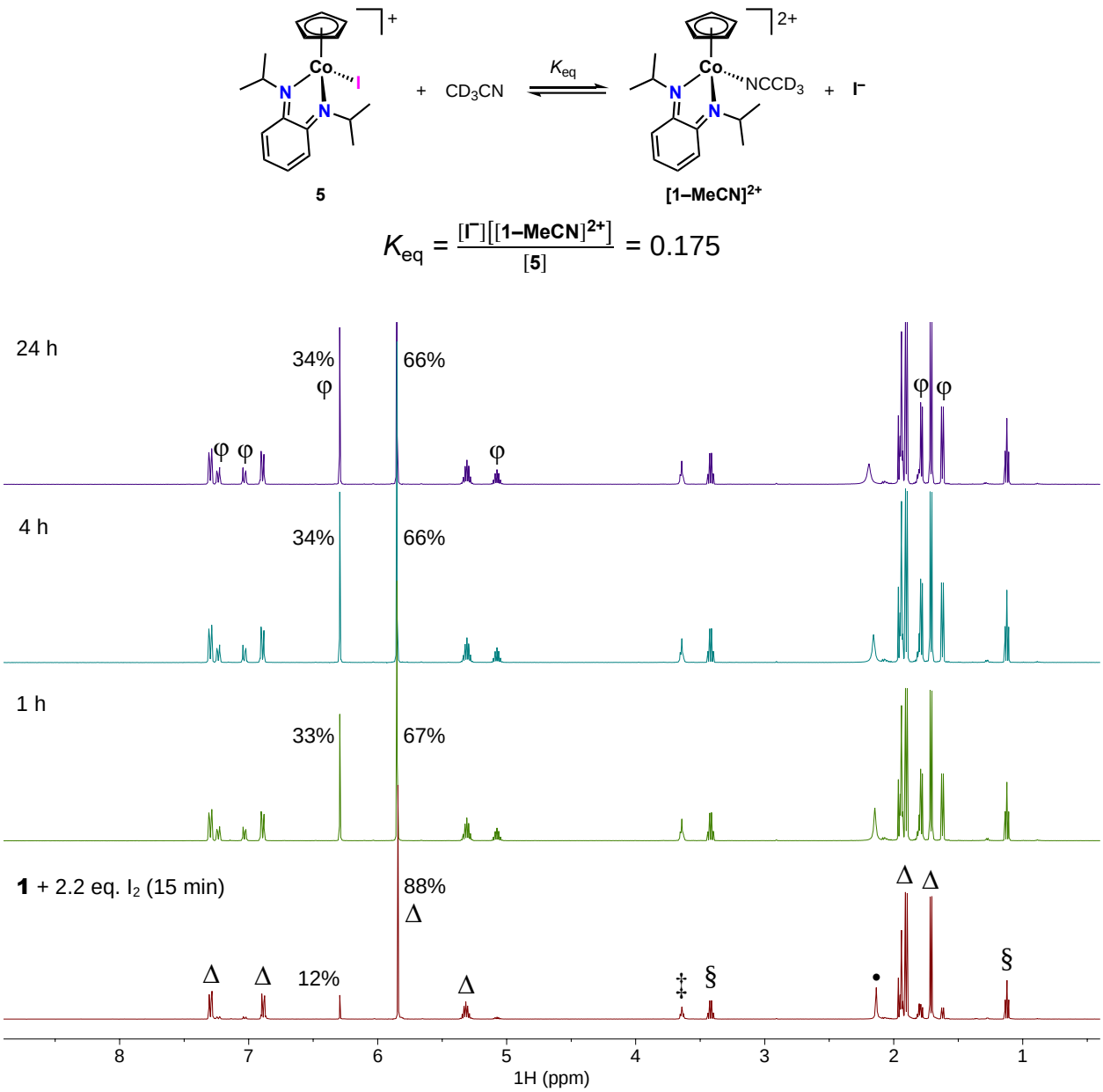

Figure S22. Monitoring the reaction of complex **1** and 2.2 equiv. I_2 in CD_3CN by ^1H NMR over 24 h. Δ = **5**. φ = **[1–MeCN]$^{2+}$**. Percentages of **5** and **[1–MeCN]$^{2+}$** based on integrations of the corresponding Cp signal. An equilibrium is reached between **5** and **[1–MeCN]$^{2+}$** in ca. 1 h. ‡ = THF. § = Et_2O. • = H_2O.

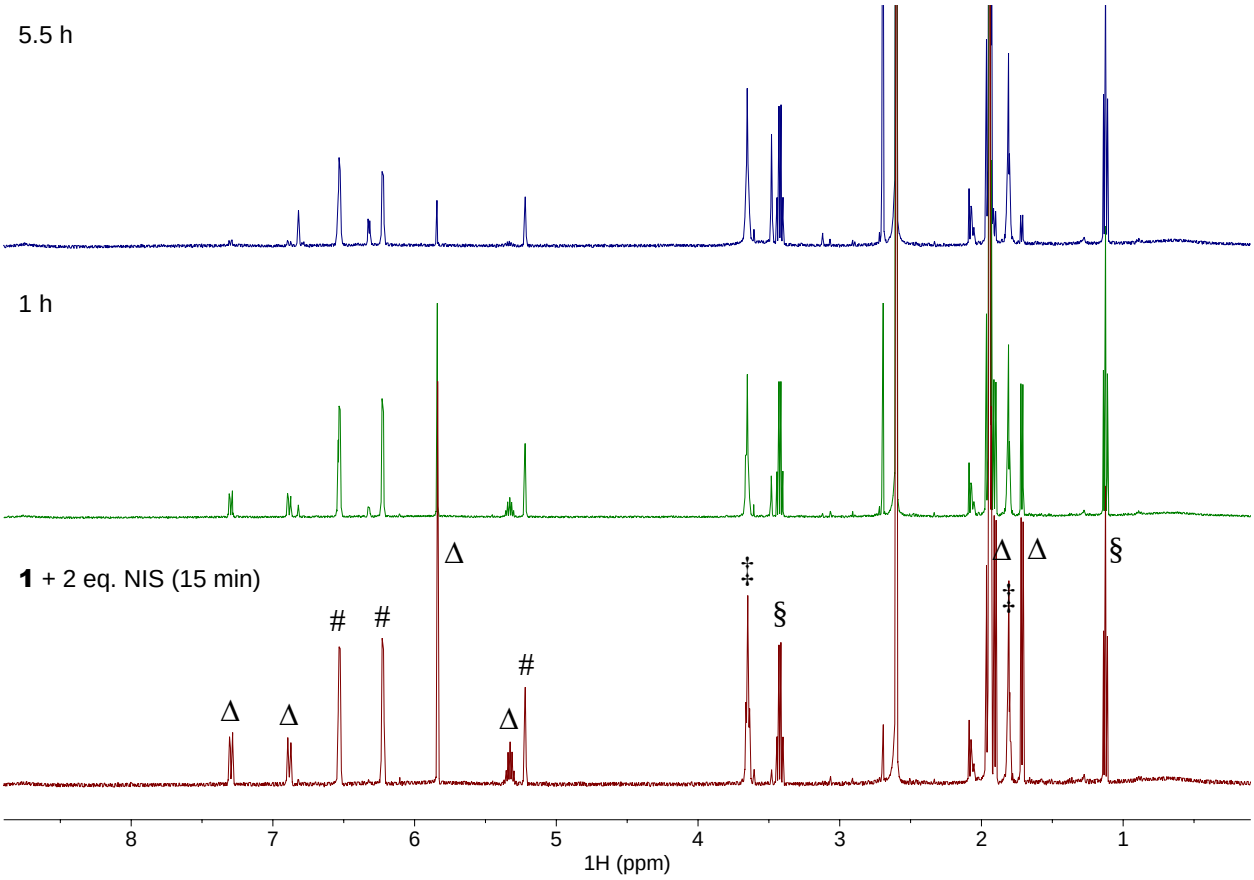

Figure S23. Monitoring the reaction of complex **1** and 2 equiv. *N*-iodosuccinimide in CD_3CN by ^1H NMR. Δ = **5**, which was slowly decomposes in solution likely due to the unstable anion. ‡ = THF. § = Et_2O. # = unknown.

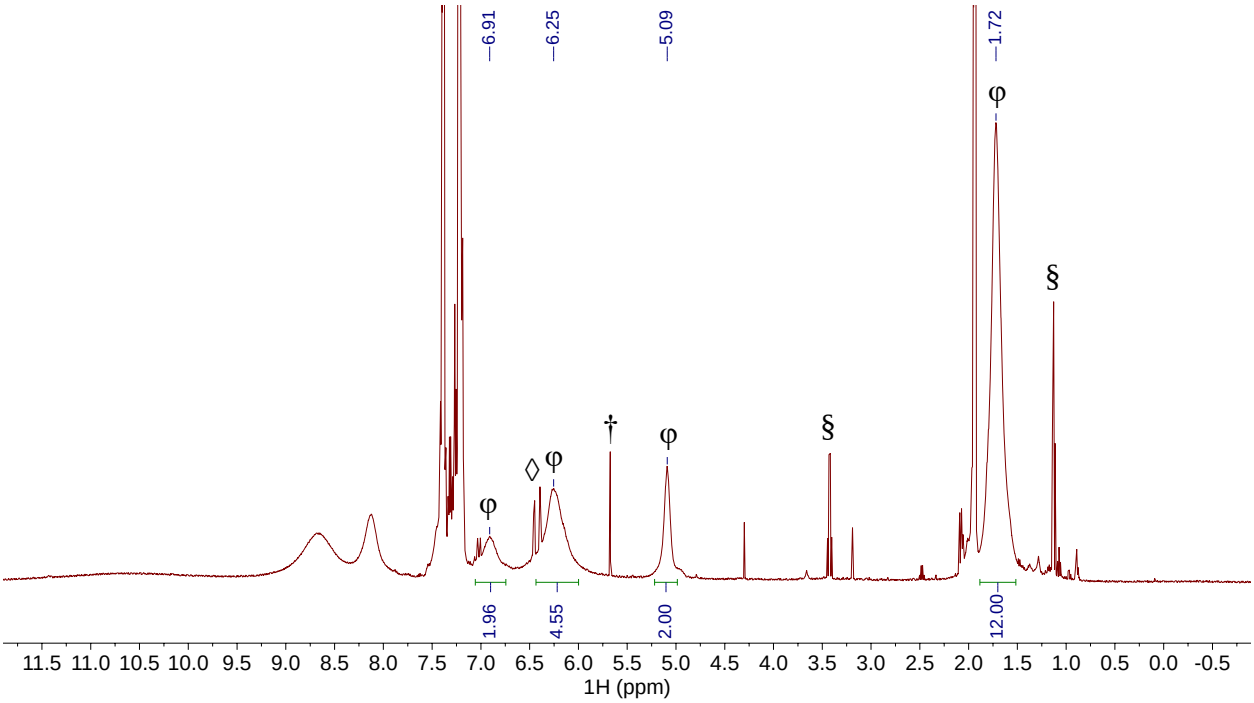

Figure S24. ^{1}H NMR spectrum for the mixture of trityl tetrafluoroborate and freshly prepared **4**. φ = **[1–MeCN]$^{2+}$**. ◊ = CpD. † = $[Cp_2Co]^+$. § = Et_2O.

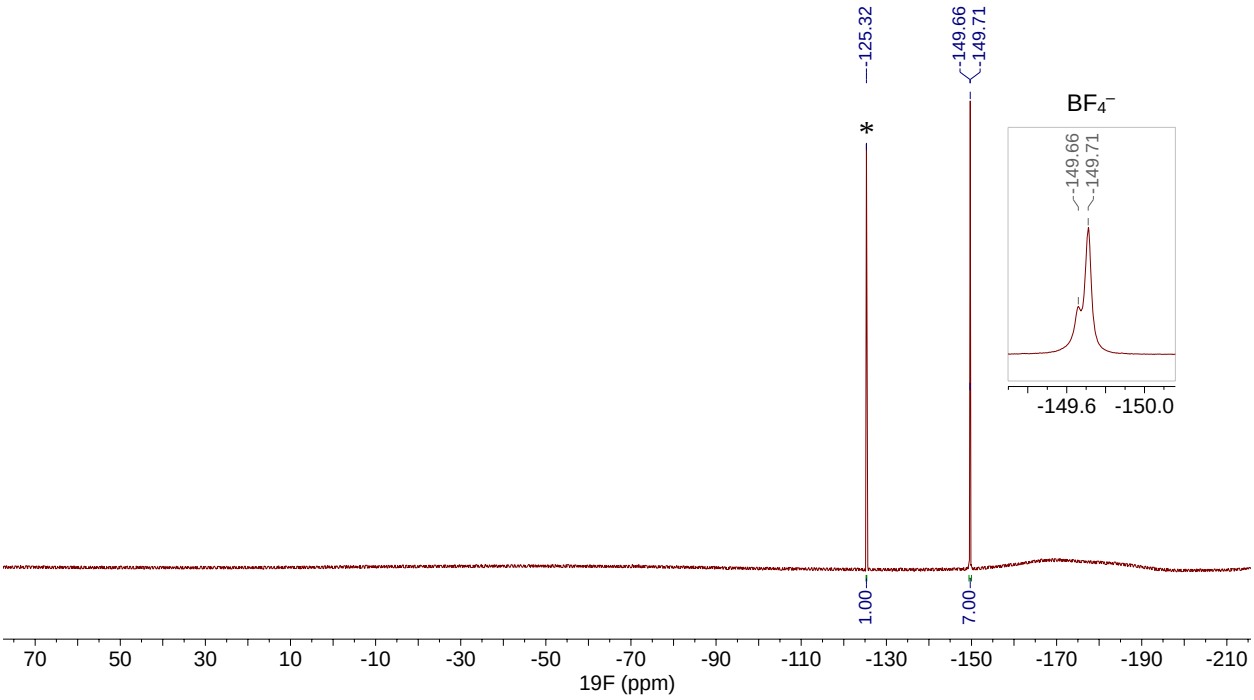

Figure S25. ^{19}F NMR spectrum for the mixture of trityl tetrafluoroborate and freshly prepared **4**. * = Ph_3C–*F*.

Electronic Absorption Spectra

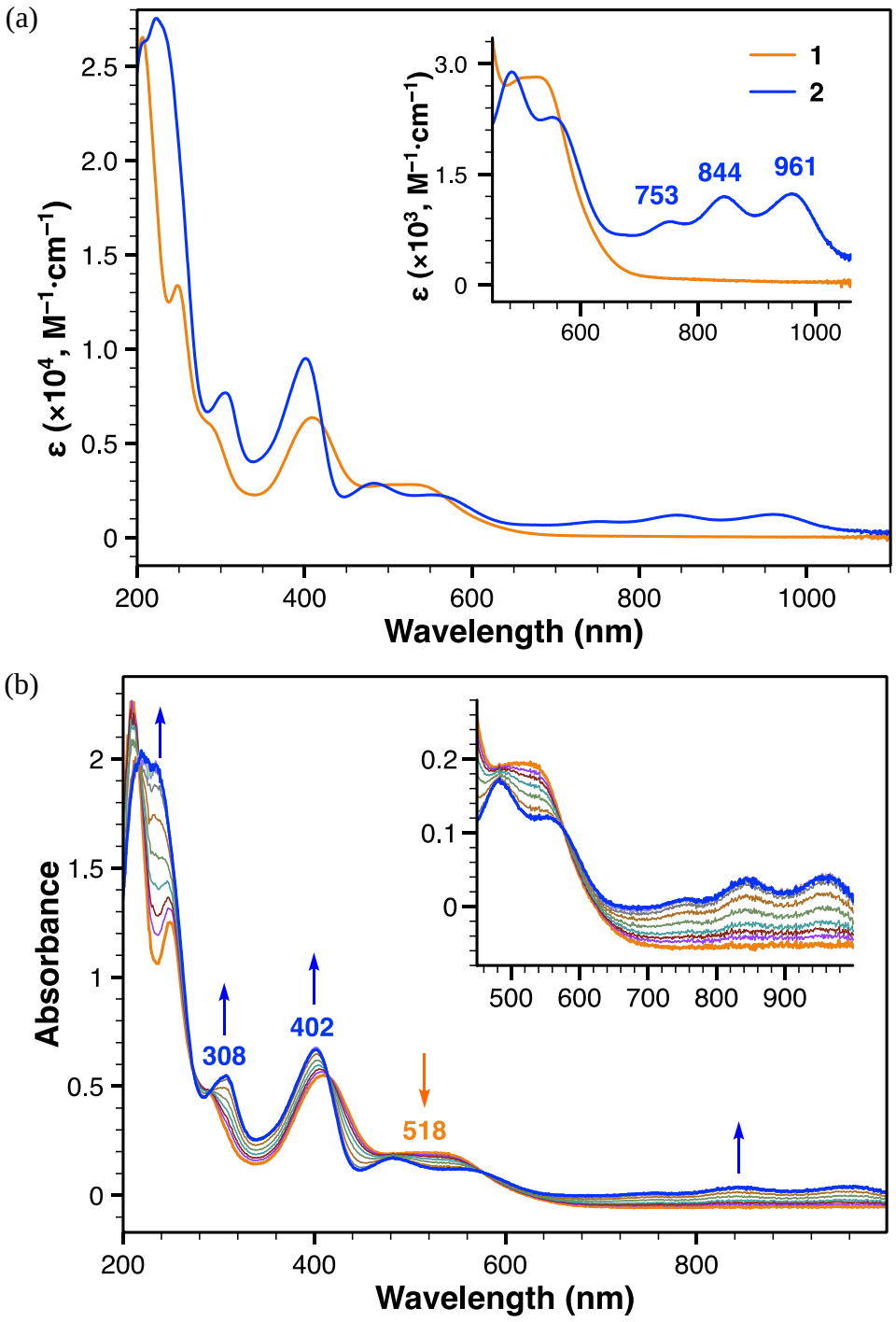

Figure S26. Electronic absorption spectra of **1** and **2** in MeCN. (a) Electronic absorption spectra of isolated **2** and **3** in MeCN. (b) UV-vis SEC studies of **2** (orange trace) in MeCN in 0.2 M [^{n}Bu$_4$N][PF$_6$] employing Linear Sweep Voltammetry to scan to negative working electrode potentials at scan rate (1 mV/s).

Cyclic Voltammetry (CV) Studies

Table S3. Electrochemical parameters for **2** in MeCN (V versus $Fc^{+/0}$, 0.1 M [^{n}Bu$_4$N][PF$_6$] as the supporting electrolyte).

v (V/s)	First 1e$^-$ Reduction Feature				
	$E_{p,a}$	$E_{p,c}$	ΔE_p	$E_{1/2}$	$i_{p,c}/i_{p,a}$
0.025	-0.589	-0.655	0.066	-0.622	1.02
0.050	-0.589	-0.655	0.066	-0.622	1.01
0.100	-0.592	-0.658	0.066	-0.625	1.00
0.200	-0.588	-0.660	0.072	-0.624	0.98
0.400	-0.583	-0.662	0.079	-0.623	0.99
0.800	-0.576	-0.670	0.094	-0.623	1.02
0.1205	-0.563	-0.683	0.120	-0.623	1.03

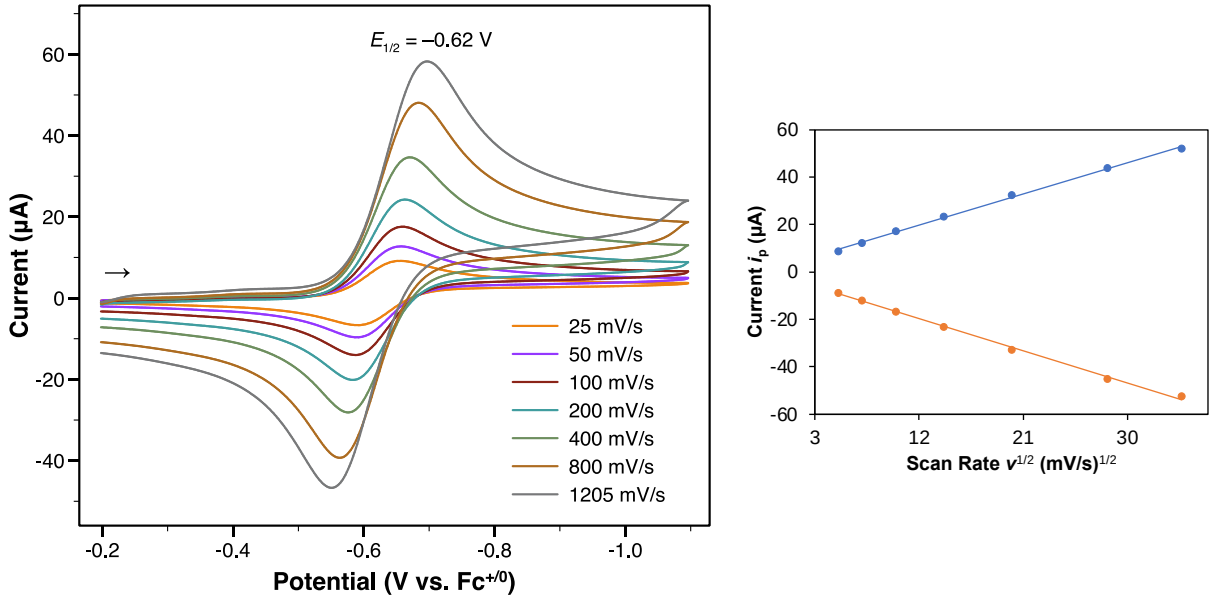

Figure S27. *Left*: Cyclic voltammograms for **2** (1 mM) in MeCN with 0.1 M [^{n}Bu$_4$N][PF$_6$] as supporting electrolyte at various scan rates. *Right*: Plots of peak current versus $v^{1/2}$ for the first 1e$^-$ reduction.

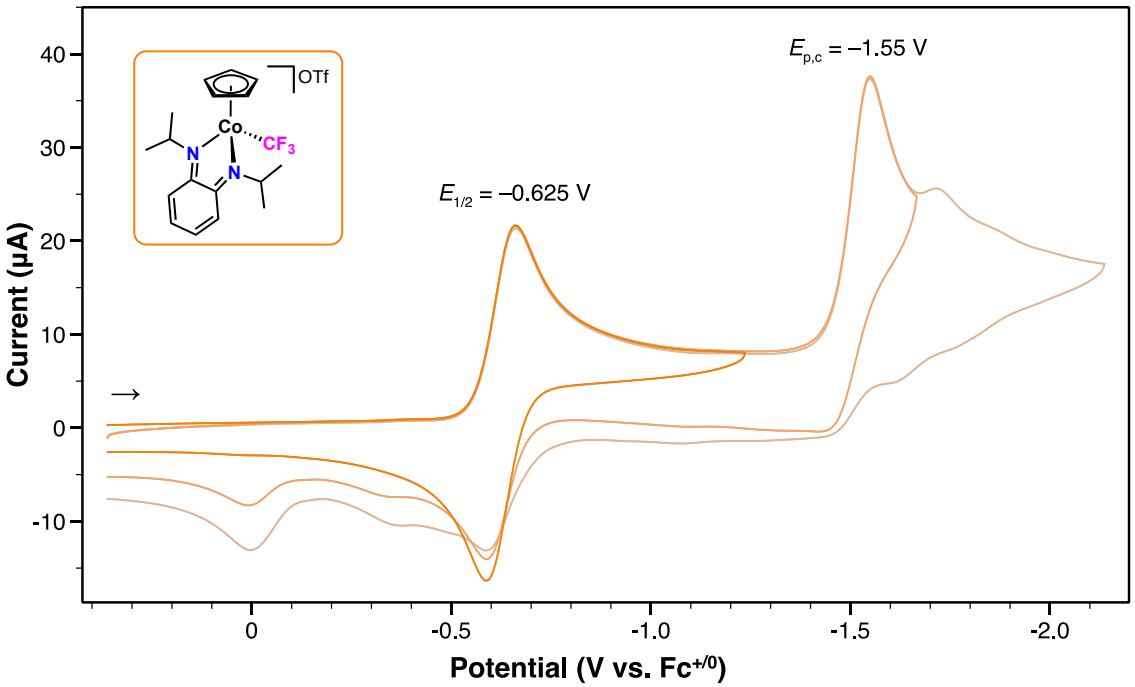

Figure S28. CV studies of **2** (1 mM) in MeCN with 0.1 M [^{n}Bu$_4$N][PF$_6$] as the supporting electrolyte at 100 mV/s.

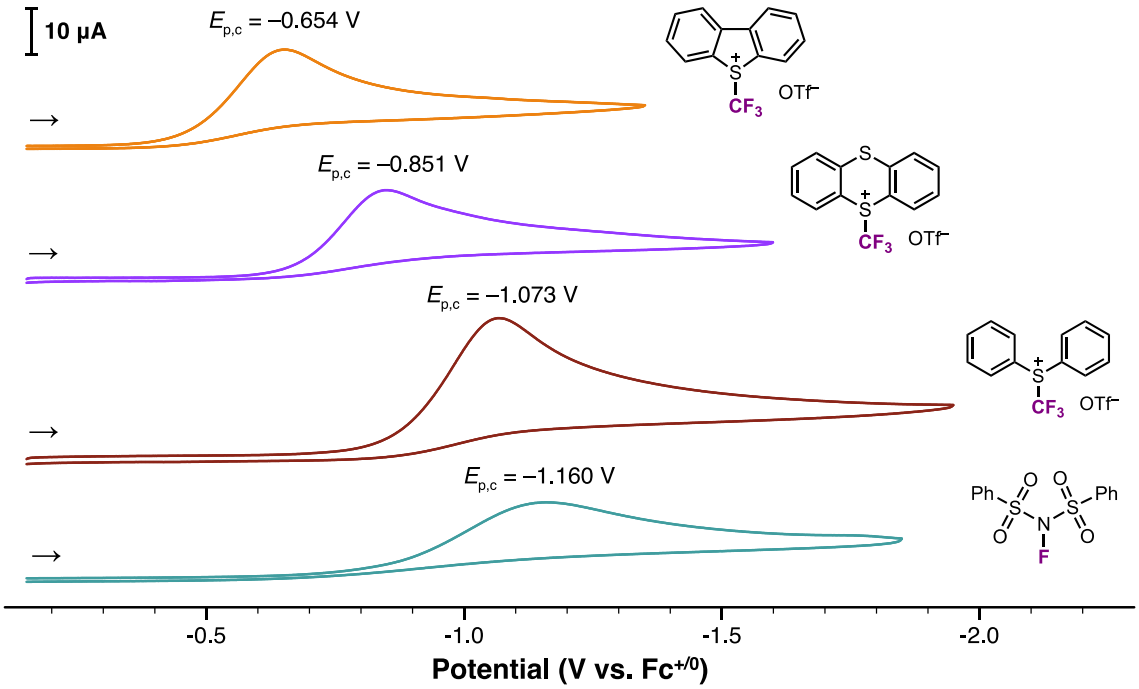

Figure S29. CV studies of three CF_3^+ reagents and NFSI (1 mM) in MeCN with 0.1 M [^{n}Bu$_4$N][PF$_6$] as the supporting electrolyte at 100 mV/s. Although not shown here, a second reduction feature for NFSI was observed at $E_{p,c}$ = –2.20 V.

Mass Spectra

(a)

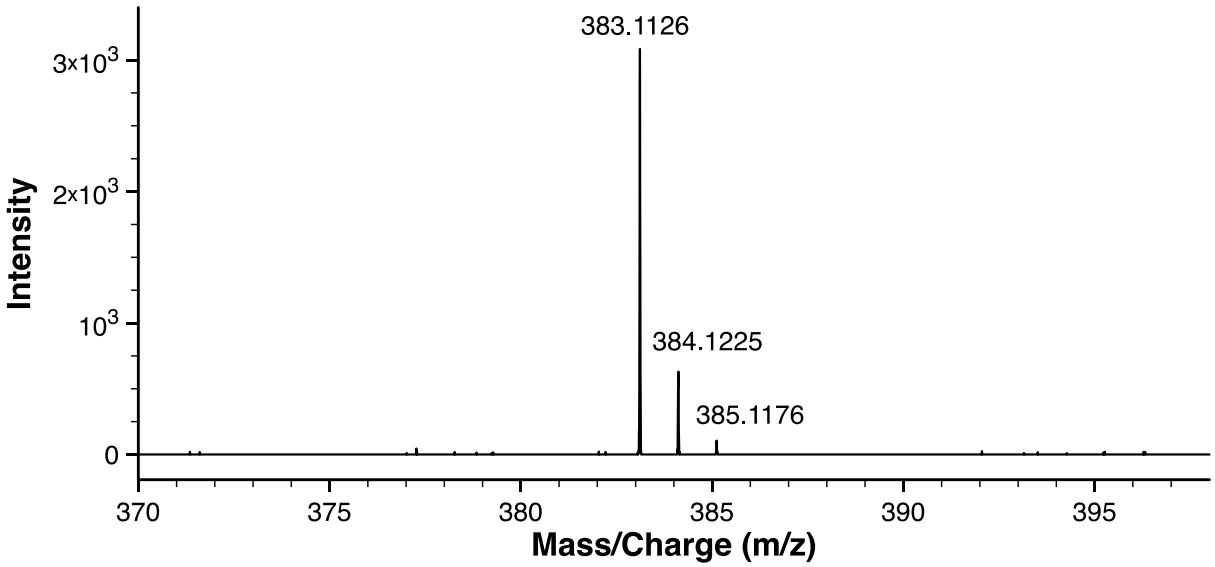

(b)

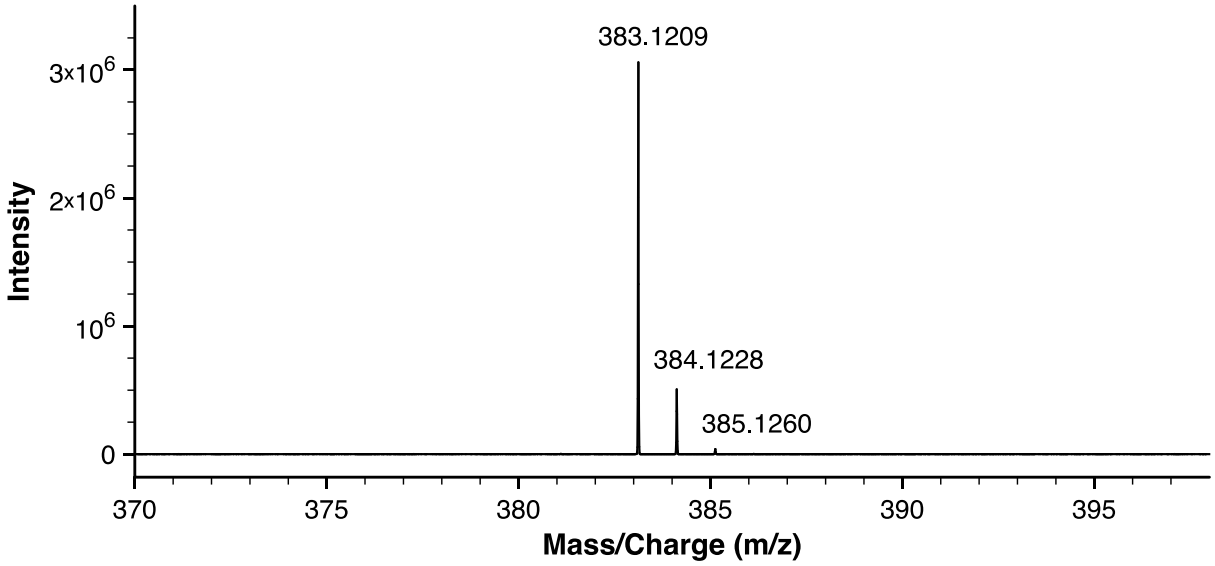

Figure S30. Mass spectra of (a) **2** and (b) **3** collected using an electrospray ionization (ESI) source on positive ion mode.

Electron Paramagnetic Resonance (EPR) Spectra

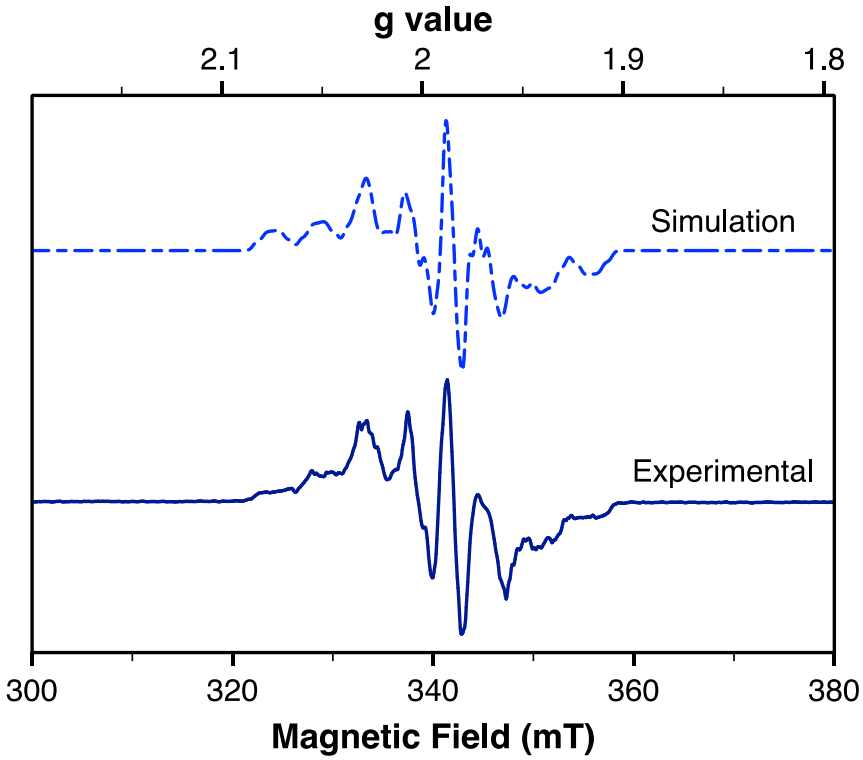

Figure S31. Experimental (solid line) and simulated (dashed blue) EPR spectra of **3** (1.65 mM) in toluene at 77 K. g_x = 1.9863, g_y = 1.9902, g_z = 1.9940. A(^{14}N) = 14.8, 18.7, 19.0 MHz, A(^{14}N') = 1.9, 24.9, 28.7 MHz, A(^{59}Co) = 55.7, 17.5, 126.6 MHz. Linewidth = 0.7 mT.

Infrared (IR) Spectra

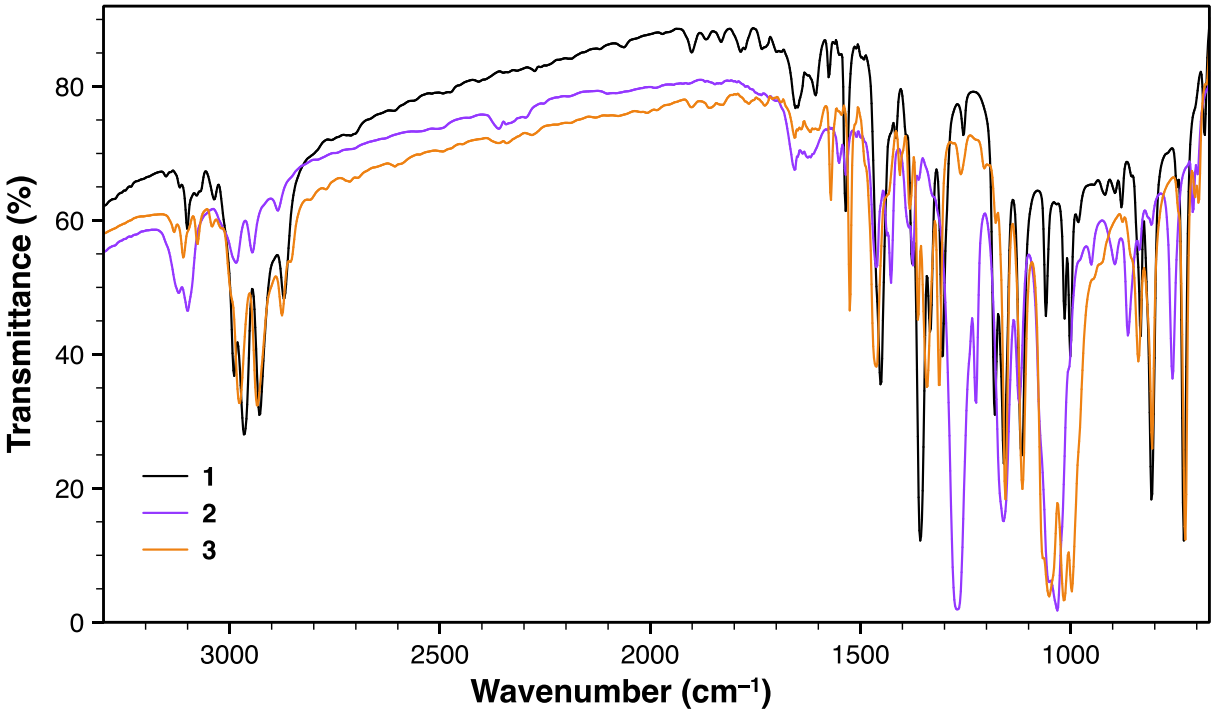

Figure S32. IR Spectra of complexes **1-3** (KBr pellet) in the region of 3300-670 cm^{-1}.

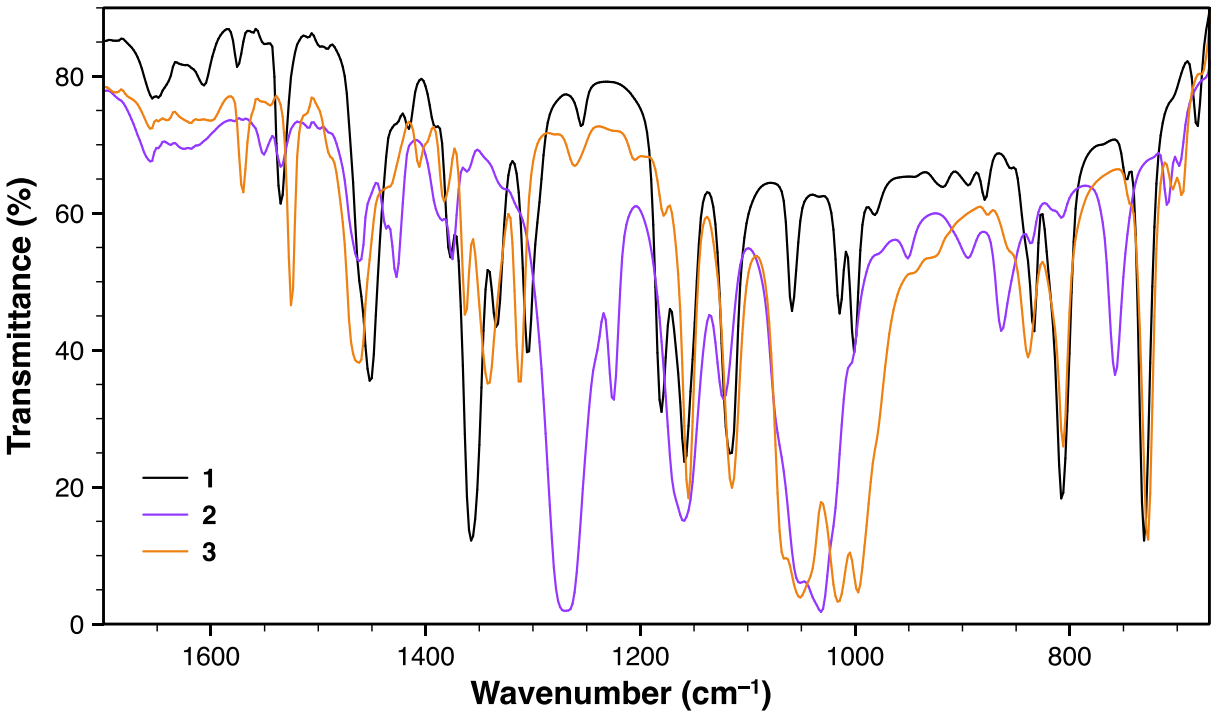

Figure S33. IR Spectra of complexes **1-3** (KBr pellet) in the region of 1700-670 cm^{-1}.

DFT Computational Results

Spin Density Map of 3

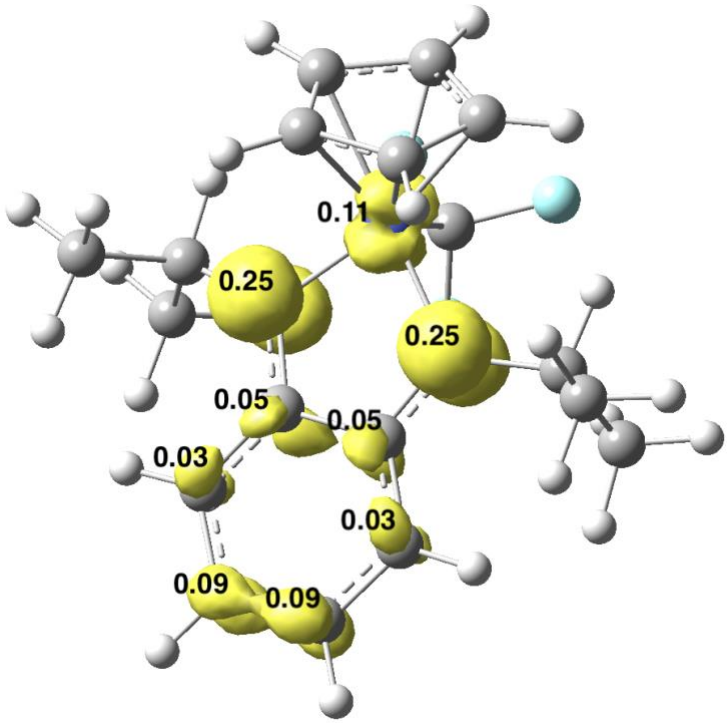

Figure S34. Mulliken spin density plot (isovalue = 0.005) of [CpCo(^{iPr}s-bqdi)(CF_3)] **3** using BP86/def2TZVP(C,H,N,O)/def2TZVPP(Co).

Optimized Cartesian Coordinates

3 (Spin = 1/2)

Co	0.98389100	-0.00000200	-0.31442200
F	1.98054100	-1.09873600	2.03918800
F	1.98054900	1.09872500	2.03918800
F	0.12687100	0.00000200	2.37816500
N	-0.42855700	1.27988000	-0.17485400
N	-0.42856100	-1.27987900	-0.17485500
C	-1.66285400	0.72814900	-0.22040000
C	-2.91120100	1.41117100	-0.25815500
H	-2.93706500	2.49784100	-0.27220700
C	-4.10300900	0.70569600	-0.30328800
H	-5.04847600	1.24960400	-0.34683600
C	-4.10301200	-0.70568300	-0.30328800
H	-5.04848100	-1.24958700	-0.34683500
C	-2.91120700	-1.41116100	-0.25815400
H	-2.93707400	-2.49783200	-0.27220500
C	-1.66285700	-0.72814400	-0.22040000
C	-0.18215700	2.71386000	0.07807000
H	0.90433000	2.77802000	0.22526800
C	-0.80718800	3.23137700	1.38779800
H	-1.90232300	3.28903700	1.34842400
H	-0.42306100	4.24241400	1.59226300
H	-0.52825200	2.58254300	2.22796500
C	-0.51777800	3.60662600	-1.13278300
H	-0.00888000	3.24919100	-2.03910000
H	-0.17899900	4.63531300	-0.93619300
H	-1.59436500	3.64185200	-1.34604800
C	-0.18216600	-2.71386000	0.07806900
H	0.90432100	-2.77802500	0.22526800
C	-0.80719900	-3.23137700	1.38779600
H	-0.52826100	-2.58254300	2.22796400
H	-0.42307400	-4.24241400	1.59226100
H	-1.90233400	-3.28903400	1.34842300
C	-0.51779000	-3.60662300	-1.13278500

H	-1.59437600	-3.64184300	-1.34605100
H	-0.17901500	-4.63531300	-0.93619600
H	-0.00888900	-3.24919000	-2.03910100
C	1.69372800	-0.70536600	-2.26723700
H	1.10914700	-1.33791700	-2.92947900
C	2.53827600	-1.15501000	-1.19416900
H	2.75874000	-2.18652000	-0.93504600
C	3.07972900	-0.00001000	-0.55755700
H	3.75342100	-0.00001700	0.29410400
C	2.53828500	1.15500200	-1.19415800
H	2.75875800	2.18650800	-0.93502600
C	1.69373400	0.70537300	-2.26723100
H	1.10915900	1.33793600	-2.92946700
C	1.25602600	-0.00000300	1.60392300

References

1. M. Zou, T. J. Emge and K. M. Waldie, Two-Electron Redox Tuning of Cyclopentadienyl Cobalt Complexes Enabled by the Phenylenediamide Ligand. *Inorg. Chem.*, 2023, **62**, 10397-10407.
2. S. Stoll and A. Schweiger, EasySpin, a comprehensive software package for spectral simulation and analysis in EPR. *J. Magn. Reson.*, 2006, **178**, 42-55.
3. G. M. Sheldrick, *SADABS*, Version 2.05, University of Göttingen: Göttingen, Germany, 2002.
4. *CrysAlisPRO*, Version 1.171.41, Rigaku Oxford Diffraction: Yarnton, England, 2018.
5. G. Sheldrick, SHELXT – Integrated space-group and crystal-structure determination. *Acta Crystallogr., Sect. A*, 2015, **71**, 3-8.
6. G. Sheldrick, Crystal structure refinement with SHELXL. *Acta Crystallogr., Sect. C*, 2015, **71**, 3-8.
7. M. J. Frisch, G. W. Trucks, H. B. Schlegel, G. E. Scuseria, M. A. Robb, J. R. Cheeseman, G. Scalmani, V. Barone, G. A. Petersson, H. Nakatsuji, X. Li, M. Caricato, A. V. Marenich, J. Bloino, B. G. Janesko, R. Gomperts, B. Mennucci, H. P. Hratchian, J. V. Ortiz, A. F. Izmaylov, J. L. Sonnenberg, Williams, F. Ding, F. Lipparini, F. Egidi, J. Goings, B. Peng, A. Petrone, T. Henderson, D. Ranasinghe, V. G. Zakrzewski, J. Gao, N. Rega, G. Zheng, W. Liang, M. Hada, M. Ehara, K. Toyota, R. Fukuda, J. Hasegawa, M. Ishida, T. Nakajima, Y. Honda, O. Kitao, H. Nakai, T. Vreven, K. Throssell, J. A. Montgomery Jr., J. E. Peralta, F. Ogliaro, M. J. Bearpark, J. J. Heyd, E. N. Brothers, K. N. Kudin, V. N. Staroverov, T. A. Keith, R. Kobayashi, J. Normand, K. Raghavachari, A. P. Rendell, J. C. Burant, S. S. Iyengar, J. Tomasi, M. Cossi, J. M. Millam, M. Klene, C. Adamo, R. Cammi, J. W. Ochterski, R. L. Martin, K. Morokuma, O. Farkas, J. B. Foresman and D. J. Fox, *Gaussian 16*, Version Revision A.03, Gaussian, Inc.: Wallingford CT, 2016.
8. F. Weigend and R. Ahlrichs, Balanced basis sets of split valence, triple zeta valence and quadruple zeta valence quality for H to Rn: Design and assessment of accuracy. *Phys. Chem. Chem. Phys.*, 2005, **7**, 3297-3305.
9. M. C. Leclerc, J. M. Bayne, G. M. Lee, S. I. Gorelsky, M. Vasiliu, I. Korobkov, D. J. Harrison, D. A. Dixon and R. T. Baker, Perfluoroalkyl Cobalt(III) Fluoride and Bis(perfluoroalkyl) Complexes: Catalytic Fluorination and Selective Difluorocarbene Formation. *J. Am. Chem. Soc.*, 2015, **137**, 16064-16073.